2013

Experimental Study On Thermal Performance And Visualization Of Loop Heat Pipe

Md Monir Hossain
North Carolina Agricultural and Technical State University

Experimental Study on Thermal Performance and Visualization of Loop Heat Pipe

Md Monir Hossain

North Carolina A&T State University

A thesis submitted to the graduate faculty

in partial fulfillment of the requirements for the degree of

MASTER OF SCIENCE

Department: Mechanical Engineering

Major: Mechanical Engineering

Major Professor: Dr. John Kizito

Greensboro, North Carolina

2013

The Graduate School
North Carolina Agricultural and Technical State University
This is to certify that the Master's Thesis of

Md Monir Hossain

has met the thesis requirements of
North Carolina Agricultural and Technical State University

Greensboro, North Carolina
2013

Approved by:

Dr. John Kizito Major Professor	Dr. Shamsuddin Ilias Committee Member
Dr. Mannur Sundaresan Committee Member	Dr. Samuel P. Owusu-Ofori Department Chair

Dr. Sanjiv Sarin
Dean, The Graduate School

Biographical Sketch

Md Monir Hossain was born on February 15, 1981, in Brahmanbaria, Bangladesh. He received Bachelor of Science degree in Mechanical Engineering from Bangladesh University of Engineering and Technology (BUET), Bangladesh, in 2005 with First Class Honors. He has received a number of awards and recognitions including Chevron Corporation Scholarship (2012) and Wadaran Kennedy 4.0 GPA Scholar Award (2013) at North Carolina Agricultural and Technical State University. He is also a member of Honor Society of PHI KAPPA PHI (2013). Md Monir Hossain is a candidate for Master of Science in Mechanical Engineering at North Carolina Agricultural and Technical State University in Greensboro, North Carolina.

Dedication

I would like to dedicate this work to my parents and to my wife for their support and love.

Acknowledgements

I want to thank Almighty God for His blessings throughout my life. I would like to express my deepest gratitude to my thesis advisor, Dr. John Kizito, for all his guidance, help and financial support, which have strongly contributed to the completion of the work. His thoughtful discussions have always served a source of inspiration for my engineering career. My appreciation and thanks to my colleagues who supported me throughout my research.

This research was funded by the Department of Defense through Wright-Patterson Air Force Research Laboratory Dayton, Ohio via a sub contract from United Technologies Corporation FA8650-08-D-2806 Task Order 0004, Subcontract Agreement#: 11-S590-0004-02-C18.

Table of Contents

List of Figures

List of Tables

Abstract

Thermal management is an important issue for applications that generate high heat flux. Choosing an efficient cooling technique depends on thermal performance, reliability, manufacturing cost, and prospects for minimization. Based on these grounds, loop heat pipe (LHP) is a highly efficient two-phase passive cooling system used for cooling of electronics and many critical components of spacecraft and satellite. Loop Heat Pipe (LHP) uses capillary action to circulate cooling fluid inside the loop. Pressure developed in the pores of a wick provides the driving force to circulate the fluid. LHP has superior heat transport capability and can operate at any orientation. In the present study, a loop heat pipe with flat evaporator has been designed and manufactured and an experimental study was performed to investigate the effects of various parameters on loop performance. LHP was instrumented with thermocouples to measure the loop temperature at various positions. Temperature oscillations have been observed at the startup of LHP. Performance of LHP has been evaluated at a wide range of evaporator heat loads. In order to comprehend the complex phenomenon inside LHP, the main structure of LHP has been made from transparent acrylic plastic to visualize the evaporation and the condensation process. A high-speed video camera has been utilized to visualize the operational process. Data collected from the experiment provides a significant insight into the physics of LHP operation. An analysis is presented to explain the startup process. Understanding of startup process is necessary for predicting the performance of LHP.

CHAPTER 1

Introduction

Heat generation in the electronic system has become a big concern with the advent of new technology. Recently much attention is given to the cooling system to improve the heat dissipation capability. Reliability of electronic component depends on the temperature level, which is a major challenge for thermal management. Convectional cooling system using air as a coolant is not capable of removing high heat flux. In addition, the need for cooling compact electronic system has become a big challenge for these traditional systems. Two-phase cooling systems such as Spray cooling, Heat Pipe (HP), Capillary Pumped Loop (CPL), and Loop Heat Pipe (LHP) have great potential to meet future challenges. All the technology mentioned above use phase change and for the passive system, the working fluid can circulate in the loop without any external mechanical pump.

Cooling device like heat pump has been used extensively for several decades due to its effective solution to thermal problems. Continuous research has been performed to improve the performance of heat pipe, which has guided to the invention of Loop Heat Pipe (LHP). LHP is a one kind of heat pipe where the evaporator and condenser components are separated. LHP's application gained its popularity after showing the successful operational capability in space programs in 1990s. LHP is a passive device which can operate in any orientation and capable of self-starting. Widespread research is going on to improve the performance and miniaturization to provide the higher cooling capability effectively. Due to the compactness of the system, now LHP is successfully used in cooling of laptops and desktops. Now the big challenge for the engineers is to increase the cooling capacity by keeping the size as compact as possible. It is very critical to cool the small surface area with high heat flux. Device as loop heat pipe (LHP)

can be an excellent solution for the problem. Investigation has shown that LHP can be effectively used for thermal management of compact electronic system (Singh, Akbarzadeh, Dixon, Mochizuki, & Riehl, 2007). Yury F Maydanik, Vershinin, Korukov, and Ochterbeck (2005) had developed miniature cylindrical LHP for electronic cooling applications. Development and improvement of the performance is the great interest of many researchers.

1.1 Specific Objectives

Experiments have been performed in different operating condition, with different kinds of working fluid and various wick structures to achieve optimum heat flux removal capability. The two-phase phenomenon present in the system makes the mechanism complex. An extensive literature review shows that not too many experiments have been performed to understand the effects of wide range of heat load in the evaporator of loop heat pipe (Ji Li, Wang, & Peterson, 2010). Especially, it is extremely important to understand the startup and steady state operating condition in the loop at different heat load condition (Maidanik, Solodovnik, & Fershtater, 1995). The performance of LHP can be unstable at low as well as comparatively high heat load conditions. Failure of the loop can be possible for both the cases. For efficient operation of LHP, it is very important to understand the behavior of loop at different heat load, which will be presented in this study.

It is also evident from the literature review that there are very few research have been conducted on the visualization of the operation of LHP (Bartuli, Vershinin, & Maydanik, 2013). The theoretical model of LHP has been developed without any physical observation of the processes taking place inside the loop. These models are unable to provide any comprehensive picture of the system. Especially for two-phase system, it is very important to investigate the behavior of the fluid inside the evaporator and condenser where the phase changes take place.

To understand the physical phenomenon of the system, it is very important to visualize the operational process in LHP. Based upon the discussion presented above, the specific objectives are:

- To design and build a Loop Heat Pipe.
- To evaluate the performance parameters of the loop heat pipe at different heat load conditions.
- To visualize the startup and component performance of the LHP.

1.2 Organization of Thesis

The present thesis has been organized in five chapters. The first chapter provides the specific objectives of the present study and the motivation behind these specific objectives. Second chapter presents the literature review on the current knowledge base on LHP. Chapter three describes the methodologies and materials used to perform the present research. Results and discussions are presented in chapter four. Chapter five includes the conclusions and recommendation for further study.

CHAPTER 2

Literature Review

Literature review is important to understand the present knowledge base and to find the knowledge gap . Chapter 2 presents information regarding historical development of LHP and performance analysis has been done so far for the improvement of LHP.

2.1 Historical Development

Loop heat pipe is one particular kind of heat pipe. The history of heat pipes must be discussed first to understand the development process of LHP. In a heat pipe, the wick structure transports heat from evaporator to condenser. Perkins Tube is one kind of two-phase device, which was invented long before heat pipe. Perkins Tube, which is also known as thermosyphon, is an essential part of the history of the heat pipe.

2.1.1 Thermosyphon. Thermosyphon was patented by Perkins (1836). Thermosyphon is a heat transfer device where the working fluid is circulated by density difference between vapor and liquid. The method is based on natural convection and does not require a mechanical pump. When the liquid is heated, the liquid vaporizes and moves upwards in the loop where it is cooled and replaced by the cooler liquid returning by gravity. The circulation keeps on with very little hydraulic resistance. A schematic drawing of the thermosyphon is shown in figure 1 utilizing solar energy in water tank system. The design is a closed tube containing water operating in two-phase cycle. Both themosyphons and heat pipe are passive devices. In thermosyphon, the condensate returns to evaporator section by gravity but in heat pipe, the condensate returns to evaporator by capillary forces. Thermosyphon has limitation in the orientation. The boiler or evaporator should be below the condenser for thermosyphon. Normally used in heating and cooling applications such as heat pumps, water heaters, boilers and furnaces.

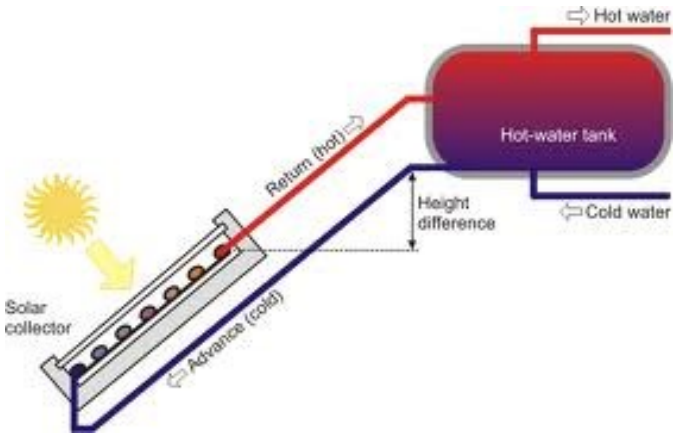

Figure 1. Schematic of thermosyphon (Gogreen Solutions Company)

2.1.2 Heat pipe. Heat pipe was patented by Gaugler (1944). During working on refrigeration system, he invented a device that can evaporate and condense a liquid without providing any external work in the system. In heat pipe, the vapor passes through the wick of the tube and releases the heat to the condenser. The process continued with capillary pressure. Use of heat pipe in space program was revived in 1962 (Trefethen, 1962). The heat pipe concept came to attention after Grover, Cotter, and Erickson (1964) published detail physics and operational characteristics. They have utilized different types of wick materials and working fluids in their study. Highest operating temperature of the loop was 1650 °C. Heat pipe can operate in any orientation and in micro-gravity condition without any external pump. For that reason, it became very popular in space program. Significant number of experiments has been conducted on heat pipe to meet the high cooling demand. Different design approach also has been implemented for the improvements in performance.

Wicking material is the heart of heat pipe through which the fluid moves. The container used for heat pipe should be sealed and evacuated. Specific amount of liquid is charged into the system to saturate the wick. Figure 2 shows three distinct regions of a heat pipe i.e. an evaporator, a condenser and an adiabatic region. The heat applied to the evaporator region turns

the liquid into vapor. The high pressure generated in the wick push the vapor through the tube to the condenser region. In the condenser, the vapor condenses and the liquid returns back to the evaporator. The pressure drop in the wick material mostly consumes the pressure generated in the wick. It is hard to transfer heat to a large distance due to high-pressure drop in the system.

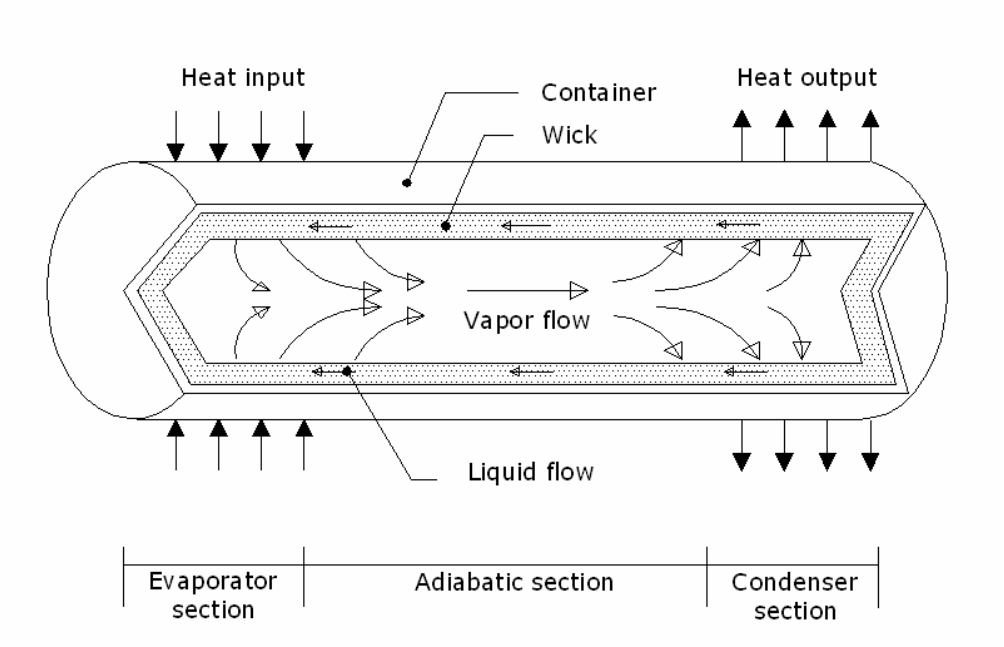

Figure 2. Schematic of heat pipe (Brocheny, 2006)

2.1.3 Capillary pumped loop. Capillary pumped loop (CPL) is very close to the structure of loop heat pipe. CPL was envisioned by Stenger (1966). CPL came into attention at the late 1970. This technology has been employed in space program to transport heat from one place to another. CPL is a two-phase passive cooling device, which uses capillary pressure developed in the wick to circulate the fluid in the closed loop. The liquid evaporates from the evaporator and condenses at the condenser. Hydraulic connection between the evaporator and the reservoir is the main difference between CPL and LHP. The reservoir is totally separated from the evaporator. However, in LHP, the reservoir is directly connected to the evaporator section. Separated reservoir in CPL has significant effects on thermal performance. The

disadvantage of the CPL is that it needs preconditioning during start up. The reservoir is heated few degree above the evaporator temperature.

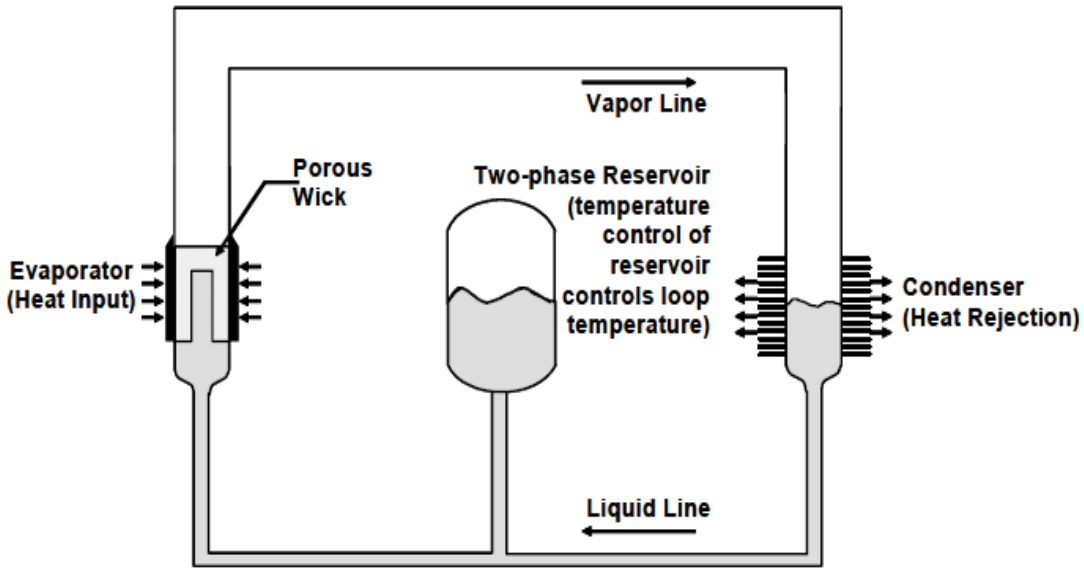

Figure 3. Schematic of capillary loop pipe (Wrenn, 2004)

2.2 Fundamental Operating Principles of Loop Heat Pipes

LHP consist of five main components. These components are

1. Evaporator

2. Compensation chamber (reservoir)

3. Condenser

4 Liquid line

5. Vapor line

Capillary force developed in the pore of the wick material is the source of the pumping action for circulating the fluid along the loop. A schematic diagram of a typical LHP is shown in figure 4. The wick is located inside the evaporator. Compensation chamber is directly connected to the wick structure of the evaporator. The compensation chamber provides accommodation for excess liquid in the loop and provides constant supply of liquid to the wick.

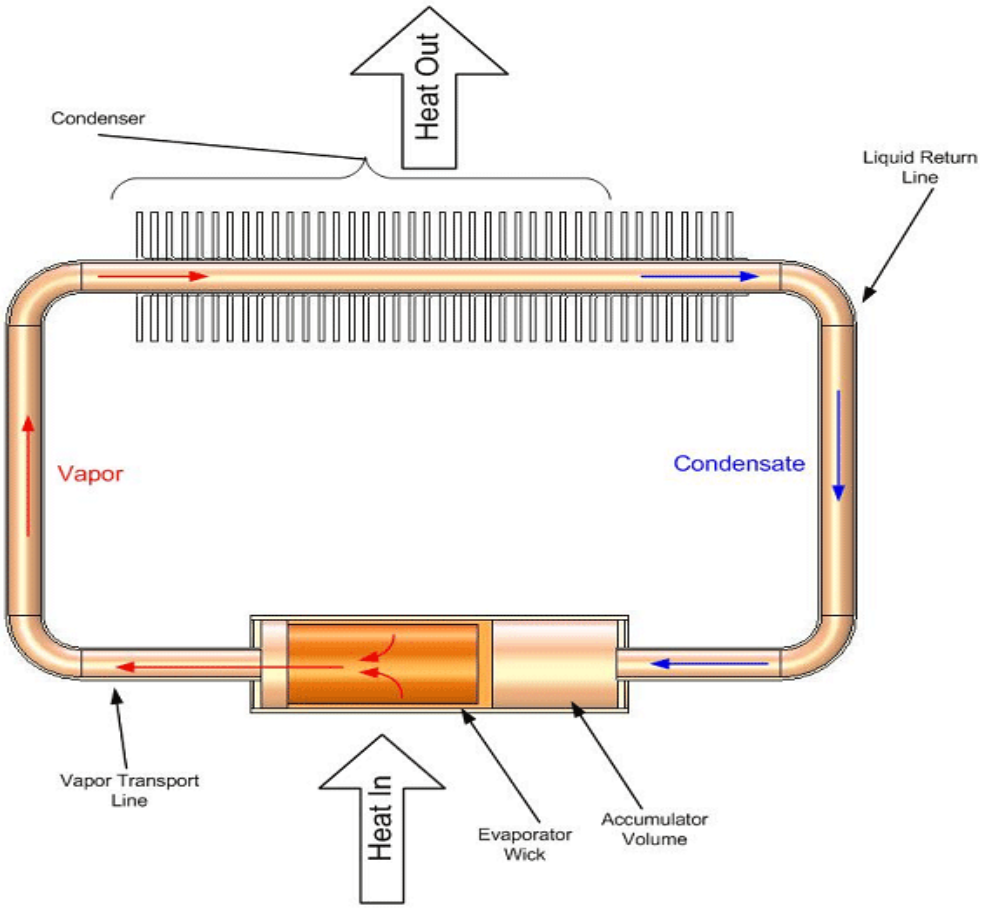

Figure 4. Schematic of LHP (Advanced Cooling Technologies Inc., USA)

When heat is applied to evaporator, the liquid in the pore of the wick is vaporizes and form meniscus in the pore. The vapor channel removes the vapor generated in the wick. Quantity of vapor depends on wick structure and amount of heat applied to the evaporator. The heat is rejected from the condenser. After the condensation, process vapor turns into liquid. The liquid then returns to the evaporator through the liquid line. The wick is normally made from sintered metal with very fine pores to increase the pumping capability. High pumping capability depends on pore size and permeability of the wick determines. LHP can operate even in micro-gravity condition efficiently. LHP can also transfer heat from heat source to heat sink at a reasonable distance.

2.3 Working Fluids

The first step in the design process of LHP is to select the working fluid. The working fluid should have the following properties

• Minimum operating temperature for phase change

•The contact angle between working fluid and porous substrates should be low. High wettability ensures maximum capillary pressure.

• The saturation pressure of the fluid at the maximum operating temperature

• The fluid should be nonhazardous and environmental friendly.

The working fluid should be compatible with the wick material. Any chemical reaction between the working fluid and the wick material will create non-condensable gas (NCG) in the system and NCG deteriorate the performance of LHP.

The common working fluids for LHP are ammonia, ethanol, acetone and water. Impact of working fluid on environment is big issue. Use of working fluid like ammonia, alcohol is decreasing due to toxicity. Nontoxic working fluid such as water as working fluid is increasing due to its thermo-physical characteristics. Water is compatible with copper and stainless steel wick. Water is also easily available and has high latent heat of vaporization. The surface tension of water is also high. The working fluid determines the temperature and pressure limit of the system. Ammonia and ethanol are used in LHP of low operating temperature and pressure. Depending on the operating temperature, LHPs are classified into four categories Faghri (1995):

1. Cryogenic (4-200 K)

2. Low (200-550 K)

3. Medium (550-750 K)

4. High (750 K and above)

Most of the LHP used for cooling purposes fall in the low and medium category temperature range. For space application, both the cryogenic and high loop heat pipe has been used.

2.4 Wick

Wick is the heart of LHP. Capillarity provides the required pressure to circulate the fluid in the system. Selection of wick material is critical for design of a LHP. Selection of the wick depends on three major properties

1. Pore radius
2. Permeability
3. Thermal conductivity

The pore radius limits the capillary pressure developed in wick. Small pore radius provides high pumping capability. A wick with small pore radius may have a low permeability. Permeability is the measure of resistance of the flow in the wick. Permeability determines the pressure drop across the wick. Low permeability offer high-pressure drop in the system. Most pressure drop takes place in the wick itself. In the design process, there has to be a compromise between porosity and permeability to minimize the pressure drop. Thermal conductivity determines the heat leak to compensation chamber. Properties mentioned above have great impact on performance of a LHP. The pore radius of the wick should be in the range of 1-100μm. The wick also should have high permeability and low thermal conductivity.

2.5 Compensation Chamber

Compensation chamber is an integral part of loop heat pipe. It is directly connected to the wick. The conventional shape of compensation chamber is cylindrical. Now there is diversity in designs. Figure 5, 6 and 7 illustrate different combinations of evaporator and

compensation chamber. Cylindrical shape needs a saddle to apply the heat. Now experiments are conducted for miniaturization of LHP. Miniaturization affects the thermal-hydraulic link between the evaporator and the compensation chamber.

Parasitic heat to the compensation chamber increases due to reduce thermal resistance between the evaporator and the compensation chamber. Parasitic heat is the part of the applied heat load is conducted through the wick structure to the compensation chamber. Parasitic heat increases the operating temperature of LHP. Returning sub cooled liquid in the condenser reduces the temperature of the liquid inside the compensation chamber.

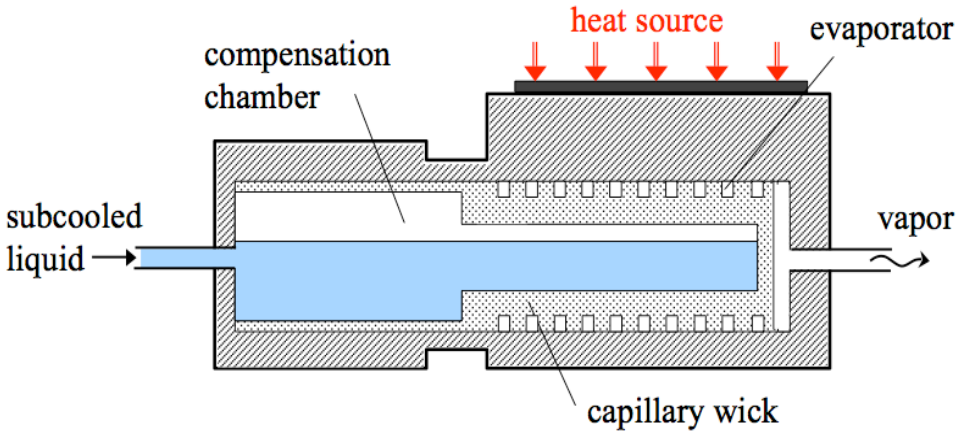

Figure 5. Evaporator/compensation chamber of cylindrical shape

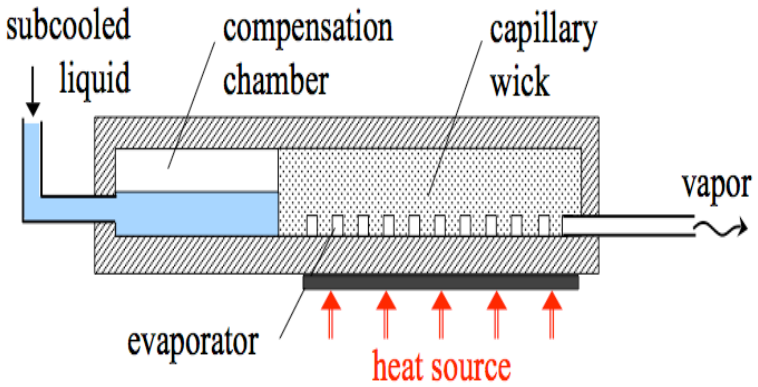

Figure 6. Evaporator/Compensation Chamber of flat shape with the reservoir located in the extension of the evaporator

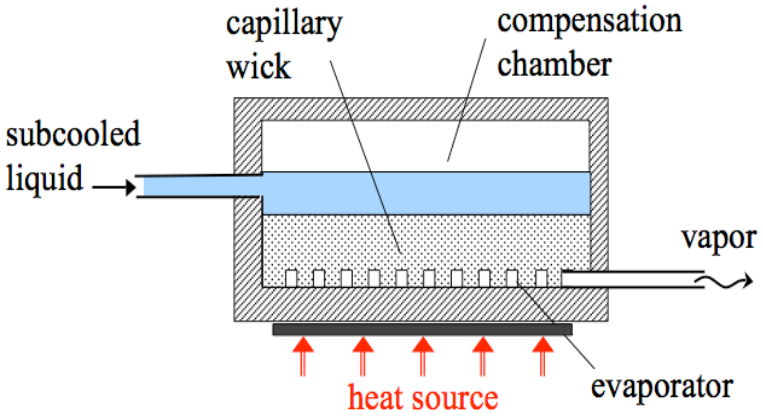

Figure 7. Evaporator/Compensation Chamber of flat shape with the reservoir located in the thickness of the evaporator

2.6 Thermodynamic Analysis of LHP:

The first step to understand the operating process of a cooling system is to perform the thermodynamic analysis of system. Thermodynamic analysis of LHP operating at steady state condition is shown in figure 8. At a steady-state condition, LHP has to satisfy mass, momentum, and energy conservation laws. However, it is difficult to maintain the energy conservation because of loss of heat from different component of LHP to environment.

The vapor generated at the evaporator wick outlet at point 1 is in a saturation state. It becomes superheated at the exit of the grooves at point 2. For a perfectly insulated vapor line, there is a negligible temperature drop in vapor line. The pressure drops in vapor line and reaches the condenser at point 3. Due to condensation, the temperature starts decreasing in condenser from point 4. The pressure drop in the condenser is small. The vapor totally condenses to liquid and starts to be sub cooled at point 5. The sub cooled liquid starts to flow in the liquid line from point 6 and keeps the temperature constant until the liquid reaches the compensation chamber at point 7. The working fluid is heated up to point 8. Thus, the energy balance is maintained in the loop.

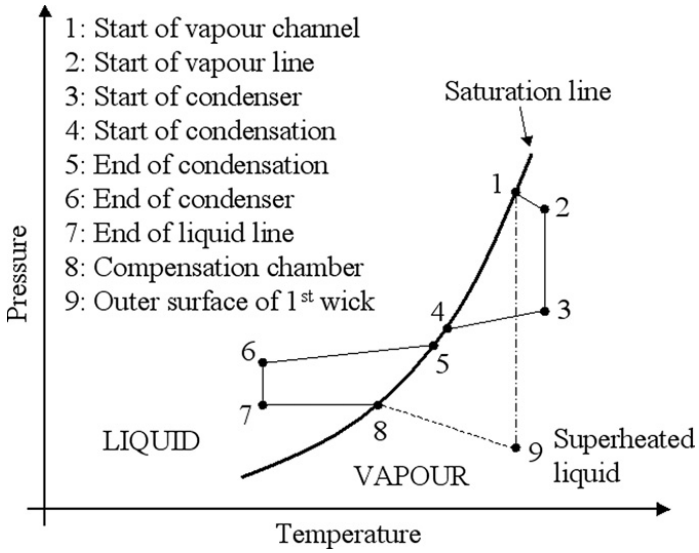

Figure 8. P –T diagram of LHP for steady-state operation (Chuang, 2003a), (Ku, 1999).

2.7 Development in LHP

Present design of the LHP is more compact than previous one. Miniaturization is very important due to compact electronic devices. Pastukhov V.G. (1999) has developed a miniature LHP of 25–30 watt heat load and it can transfer the heat up to 250 mm distance. The concept of low power management electronic cooling for spacecraft applications was also introduced by Bienert W.B. (1999). Now most of the evaporators have flat surface. Advantage of the flat surface is that it can be integrated easily into the compact electronic systems. Liquid can evaporate uniformly on the flat surface and keeps the surface isothermal.

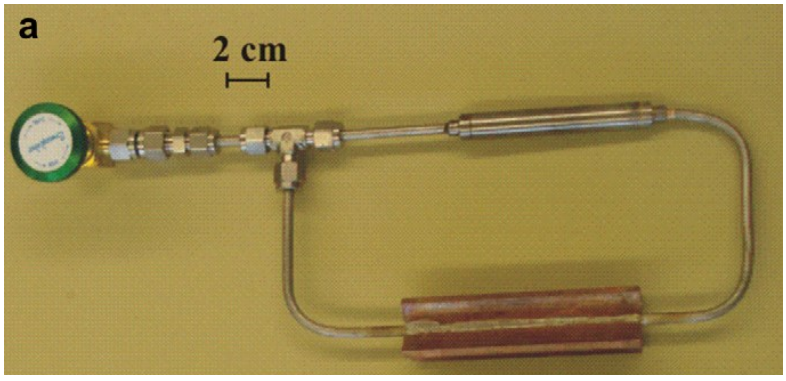

Figure 9. Loop heat pipe with cylindrical evaporator(Santos, Bazzo, & Oliveira, 2012)

Maidanik Y.F. (2000) have performed tests on LHP with heat load of 40 to 80 watt with horizontal and vertical orientations for flat disc-shaped evaporator. Tu et al. (2009) has developed a two-dimensional numerical model to characterize heat and mass transfer in the evaporator and he has also presented an experiment to verify the start-up process in LHP with flat evaporator. The effects of different working fluids on flat evaporator has been done by Liu et al. (2011). Singh, Akbarzadeh, and Mochizuki (2008) have developed a miniature flat shape copper disc evaporator with 70 watt heat capability and the temperature of the evaporator was below 100 C.

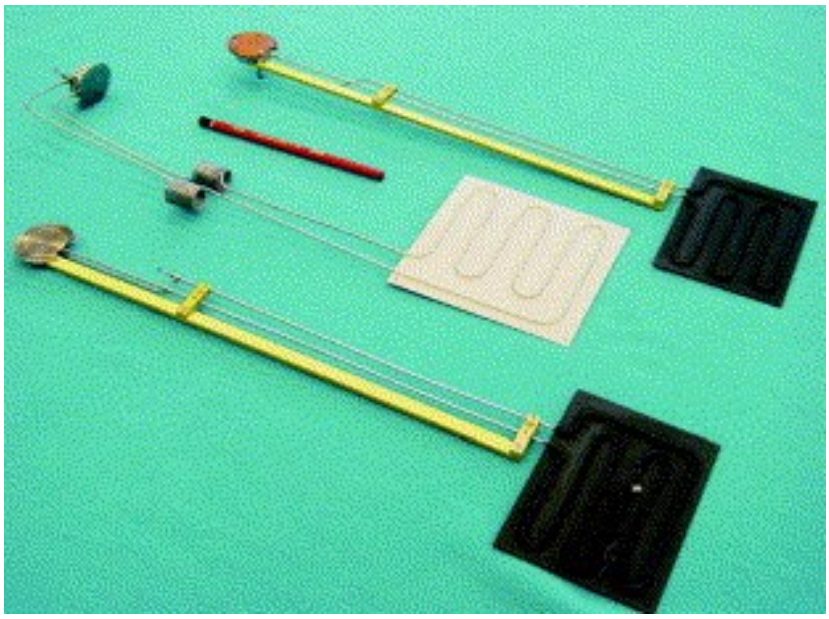

Figure 10. LHPs with flat evaporators (Yu F Maydanik, 2005)

Moon, Hwang, Yun, Choy, and Kang (2002) have designed Copper based miniature loop heat pipe was able to remove heat load of 11.5 watt from a 35X35 mm^2 area of laptop. Yury F Maydanik et al. (2005) had developed copper-water miniature cylindrical LHP with load capacity of 130 watt for electronic cooling applications. Cytrynowicz et al. (2002) have designed and fabricated Coherent Porous Silicon (CPS) MEMS loop heat pipe capable of removing high heat flux.

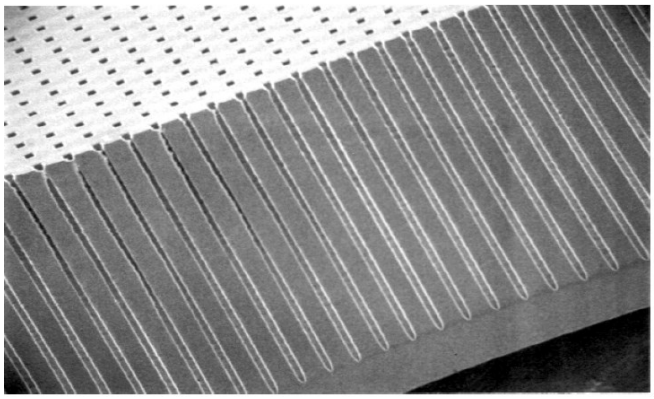

Figure 11. SEM micrograph of Coherent Porous Silicon of pore diameter 5µm (Cytrynowicz et al., 2002)

2.8 Parametric Effects of LHP

The performance of LHP is affected by numerous parameters. Effects of different parameters of LHP have to be considered during design process. The following paragraphs illustrate the effects of different parameters on performance of LHP.

2.8.1 Amount of fluid in LHP. The amount of working fluid charged into the system has no effect on the operation of LHP. However, from the thermal analysis, amount of working fluid in compensation chamber may affect the radial heat leak and can have a significant impact on the loop operation. Ku, Ottenstein, Rogers, Cheung, and Powers (2001) have investigated the effect of void fraction in evaporator with different fluid inventory and the relative tilt between the evaporator and the compensation chamber. Their test results have signified the effect of vapor void fraction inside the evaporator core for LHP operating at low heat loads. The optimum fill charge ratio and the heat flux conditions have been also investigated (Lee, Park, & Lee, 2004). In the experiment, the compensation chamber was located above the wick. They have used sintered stainless steel and brass metal wick. The working fluid is distilled water. The fill charge ratio ranged from 40 % to 60 % of total volume and the applied heat flux was varied from 1.5W/cm^2 to 5.9W/cm^2. LHP with similar configuration has been also studied by Boo and

Chung (2004). They used methanol as the working fluid and polypropylene (PP) as porous wick and did not find any significant effect of the fill charge ratio on the LHP thermal resistance (figure 12). Nevertheless, the experimental results indicate a maximum heat load for an optimum value of the fill charge ratio of 0.4–0.5.

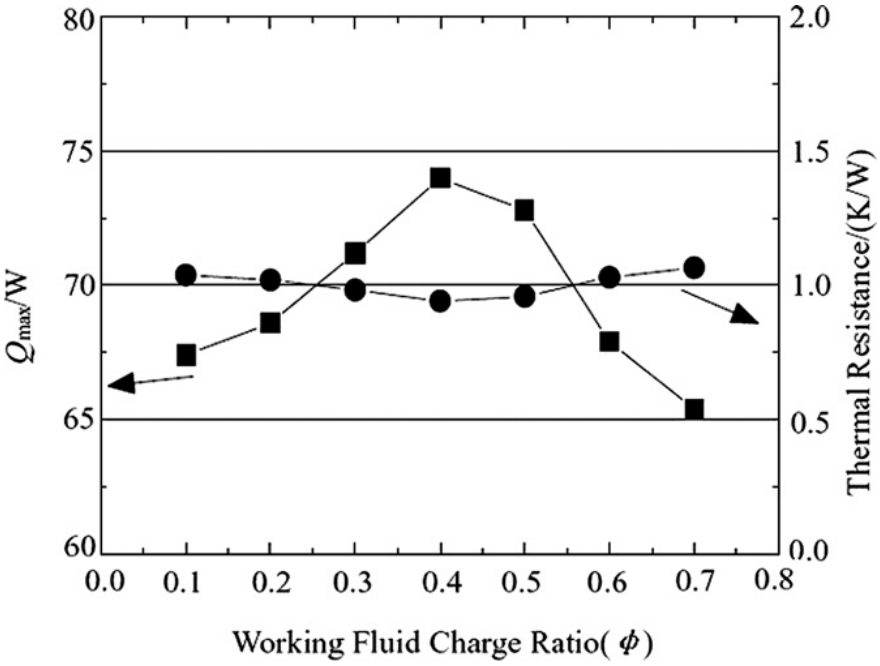

Figure 12. Q_{max} and R_t vs. working fluid fill charge ratio (Boo & Chung, 2004)

2.8.2 Effect of the porous wick characteristics. The performance of LHP is affected by three major characteristics of porous wick. They are pore diameter, porosity, the permeability, and the thermal conductivity. The small pore diameter ensures a large capillary pressure. Large porosity and permeability decreases the hydraulic resistance. Low thermal conductivity of wick minimizes the parasitic heat flux to compensation chamber. The thermal conductivity is a function of the porosity of the wick and the thermal conductivity of the liquid. Boo and Chung (2004) have used several polypropylene wicks. The pore diameters ranged from 0.5 to 25 μm. The effect of pore size on the maximum heat load and thermal resistance is shown in figure 13. From the figure, it can be seen that the maximum thermal load increased for reduction in pore

size diameter for high pressure but also have to think about permeability. For the design process the optimum value should be choose for pore size and permeability.

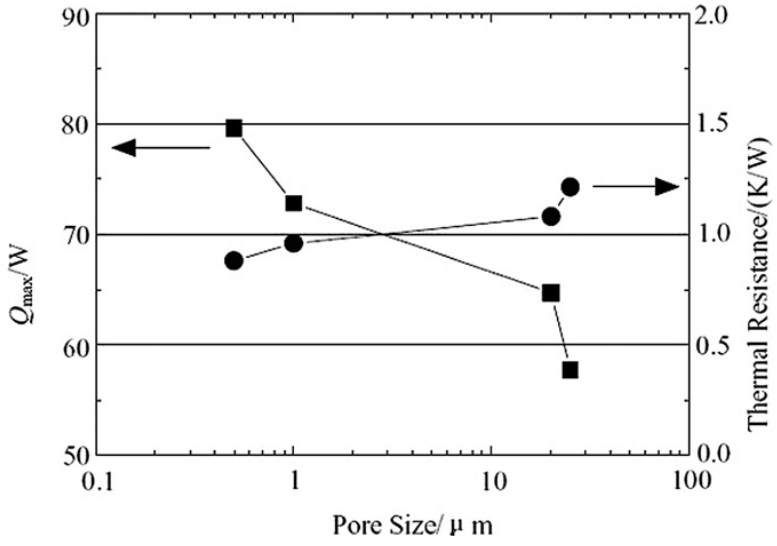

Figure 13. Q_{max} and R_{th} for various pore sizes (Boo & Chung, 2004).

Figure 14 illustrate porosity and permeability as a function of the pore diameter. In figure 14, there is a wide range of data for porosity and the permeability for a given pore size. The porosity is between 30 to 75 % and permeability is between $1x10^{-14}$ and $1x10^{-13}$ m^2 and permeability increases with the pore diameter.

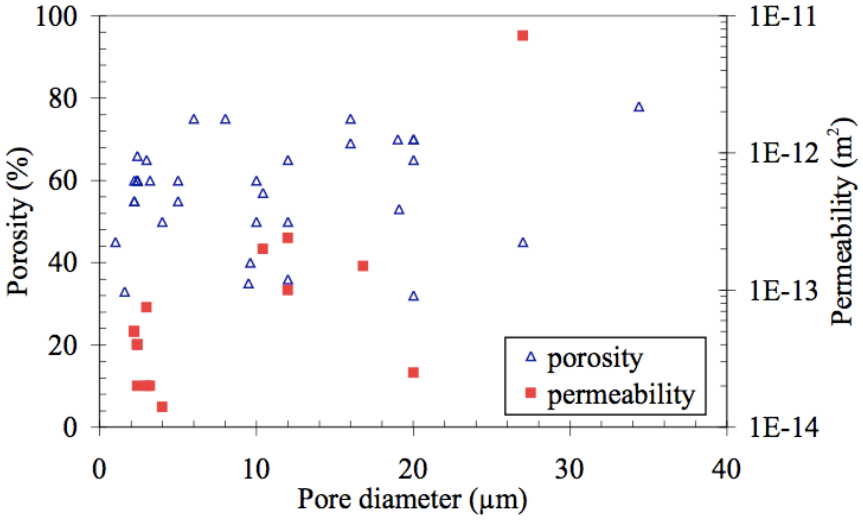

Figure 14. Properties of wicks (Hoang, O'Connell, Ku, Butler, & Swanson, 2003)

Data accumulated by Hoang et al. (2003) on porous characteristics demonstrates that permeability increases with the increase of pore diameter. The result of this study is shown in figure 15. The most utilized wicks in LHP are polyethylene, PTFE, titanium, copper, stainless Steel, brass, and nickel-chromium. The use of copper as wick has been started recently. Normally the pore diameter of wick varies between 1 and 50μm, and for copper between 20 and 100μm.

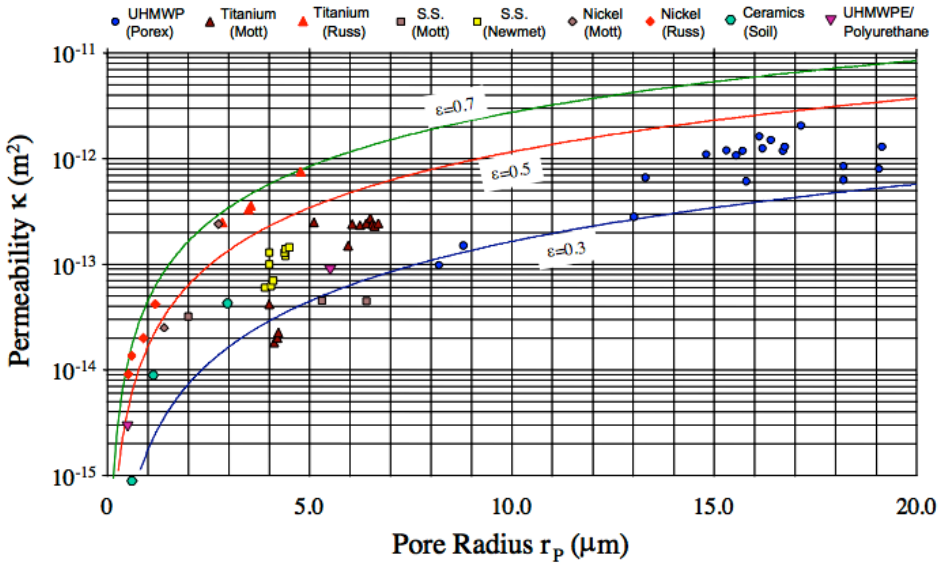

Figure 15. Properties of common wicks of LHP (Hoang et al., 2003)

Experiment has been performed to study the effect of manufacturing process on the properties of a sintered-nickel porous (Jinwang Li, Zou, Cheng, Singh, & Akbarzadeh, 2010). The study shows effect of mechanical stress applied to the sample and the concentration of microcrystalline cellulose added to the sintered-nickel porous. Biporous wick structure (Yeh, Chen, & Chen, 2009) is also developed and utilized in LHP. In the study, the average pore diameters were 7 and 24μm.

Effective thermal conductivity is very important issue because it determines the amount of heat leak from the evaporator to the compensation chamber. Effective thermal conductivity of

porous structure k_{eff} is calculated from the thermal conductivity of wick material, liquid and the porosity (Mo et al., 2006).

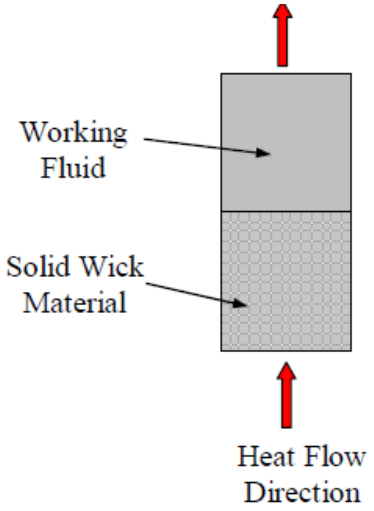

Figure 16. Schematic for effective thermal conductivity(Chuang, 2003b)

The effective thermal conductivity of the wick shown in previous figure can be calculated from the following formula

$$k_{eff} = \frac{k_{wick} k_L}{\varepsilon k_{wick} + (1-\epsilon) k_L}$$

where, K_L is the thermal conductivity of the liquid and K_{wick} is the thermal conductivity of the wick and ε is the porosity of the wick. Numerous experiments have been performed to measure and control the effective thermal conductivity. Jinwang Li et al. (2010) has calculated k_{eff} for a nickel wick of 75% porosity as 3 W/m K and for the same nickel wick with porosity of 56 %, the effective thermal conductivity was 6 W/m K (Mo et al., 2006).

2.8.3 Vapor groove. Position and shape of vapor groove can influence the heat transfer coefficient in the evaporator (Cao & Faghri, 1994; Figus, Bray, Bories, & Prat, 1999; Zhao & Liao, 2000). Vapor groove also has effect of the on the capillary and boiling limits of a LHP(Yao W., 2004). The analysis includes the number of grooves, groove width (from 0. 15 to

0. 65 mm) and the porous wick thickness (from 3 to 8 mm). They have mentioned that boiling limit increases with the number of grooves and boiling limit is at a maximum for a fin/groove width ratio of 0.5. Capillary limit increases with the fin width.

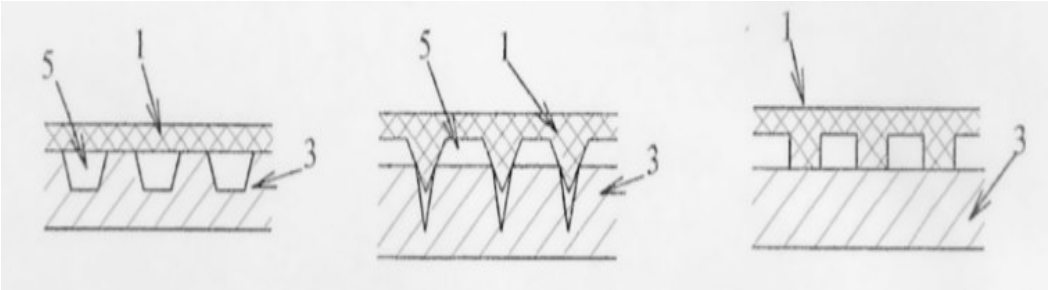

Figure 17. Design of different vapor grooves (Altman, Mukminova, & Smirnov, 2002)

Vapor channels are machined either at the inner surface of the evaporator container, or at the outer surface of the porous wick. Sometimes transverse channels are also added to longitudinal ones. Heat transfer coefficient increase for transversal micro grooves along with longitudinal grooves on wick (Platel, Fudym, Butto, & Briend, 1996). The position and the dimensions of vapor grooves depend on feasibility and to the cost of the groove machining.

2.8.4 Instrumentation. To determine the effects of different parameters, LHP is instrumented with different types of sensors. Numerous techniques are implemented to realize the accurate response of the system.

Heat flux applied by the heating element is obtained from the measurements of current, voltage or resistance. To measure the temperature, thermocouples are used in different component of LHP. Temperature is plotted against the heat flux to understand the effects of heat flux on different components of LHP. The temperature profile in the condenser distinguishes condensation region from sub cooling region. To correctly analyze the thermal profile in the condenser Bartuli et al. (2013) have installed twelve copper-constantan thermocouples OMEGA TT-T-30 along the condenser.

The most important parameter in the system is the pressure. Few experiments were conducted to measure absolute pressureKu et al. (2001); (Lee et al., 2004; Ogushi, Yao, Xu, Masumoto, & Kawaji, 2003; Singh, Akbarzadeh, & Mochizuki, 2010) in LHP.

Now researchers are more interested in visualization techniques. Visualization of LHP will explain the physics behind the operation. Neutron radiographic was used to visualize the liquid and vapor phase inside the LHP(Cimbala et al., 2004). For visualization of flow clear tubes were used in vapor and liquid line and a transparent window was made in the compensation chamber (Wang & Nikanpour, 2007). To visualize the phase changes in the evaporator, a bore scope was utilized in the compensation chamber (d'Entremont & Ochterbeck, 2008). Infrared metrology was employed to find the temperature distribution along LHP(Ji Li et al., 2010). Infrared visualization technique was also implemented to track the flow in the vapor and liquid line in LHP (Launay, 2010).

2.9 Start-up and Steady-state Operation

LHPs have reliable start-up ability. A minimum heat load is required to begin the flow in the system; where the minimum heat load requirement depends on the design and size of LHP. The startup process of LHP may fail if the minimum heat requirement is not fulfilled.

It is difficult to predict the shape of the LHP operating curve. However, the usual operating temperature versus the heat load plot shows U or flat shape. Two operating conducting mode have been described by Ku (1999). At low heat loads, condenser is only partially utilized for vapor condensation. This mode is called a variable conductance mode (VCM). The operating temperature is low in this mode. As the heat load continues to increase, the condenser can no longer dissipate the excess energy. This operating mode is called as fixed conductance mode (FCM)

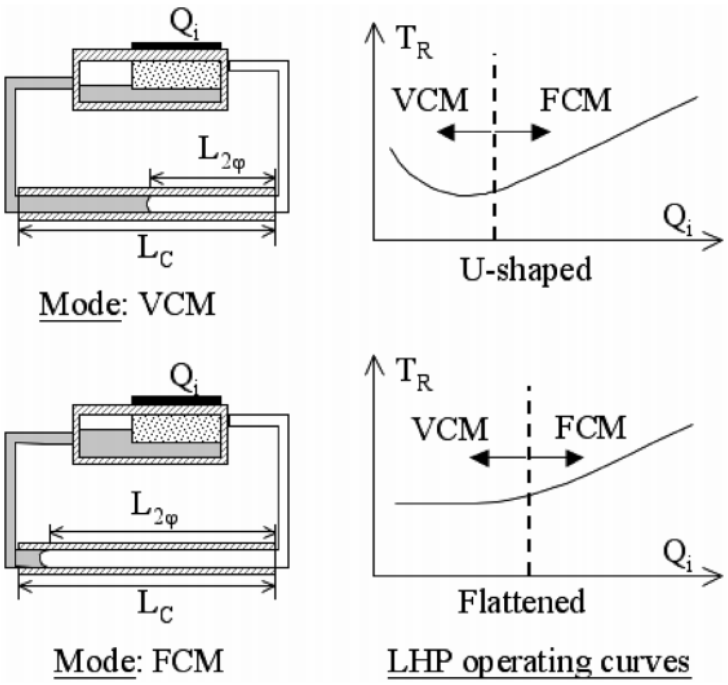

Figure 18. LHP operating curves

U-shaped curves have been observed by Y.F Maydanik (2004). Flattened shapes have been usually observed for low-thermal conductivity wicks with low-pressure working fluids such as methanol, ethanol, or acetone

The most difficult condition for LHP start-up is for liquid filled vapor channel during startup. It was found that two-phase fluid existed in the vapor channel for the small superheat case (Cheung, Hoang, Ku, & Kaya, 1998). Experiments were also performed to study low power start-up process with different orientations. The authors concluded that the required superheat, maximum temperature at start-up, and time required for start-up strongly depends on loop orientation (Kaya & Ku, 1999). Maidanik et al. (1995) have presented few possible scenarios of the inside the evaporator/compensation chamber prior to start-up. Situation 4 presents the most difficult condition for LHP start-up. Here the evaporator grooves are filled with liquid while the evaporator core contains vapor. Liquid superheat is required to begin the nucleation in the grooves.

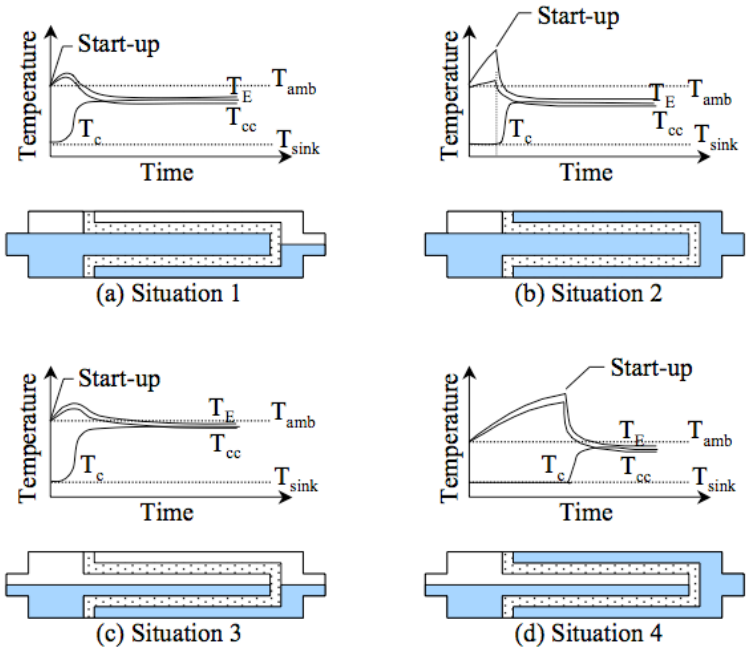

Figure 19. Four different situation for startup process (Maidanik et al., 1995)

2.10 Transient State Operation in LHP

LHP does not require pre-conditioning for starting like capillary pumped loop (CPL). It can start directly by applying heat to the evaporator. For this reason, LHP is also known as self-starting two-phase heat transport device. However, self-start does not necessarily imply a quick and immediate start. Delayed start may damage the operating system. It is very important to understand the start-up process and to highlight the parameters that influence its characteristics. During start-up, the temperatures in the vapor line increase. The sharp temperature rise is due to the vapor generation. Parameters that influence the startup process of loop heat pipe are mentioned below:

- Amount of working fluid and orientation of loop
- Characteristics of wick
- Applied heat load
- Heat sink temperature

- Working fluid

Baumann, Cullimore, Yendler, and Buchan (1999) have also mentioned effects of non-condensed gas (NCG) in LHP. Amount of applied heat load is a critical issue. If the heat load is too high, dry up can take in the wick

Experiment result of Singh et al. (2007) and Ji Li et al. (2010) regarding startup are shown in figure 20 and 21 for low heat load. Both the figures show high oscillation in temperature profile due to the instability of meniscus of the fluid in the wick.

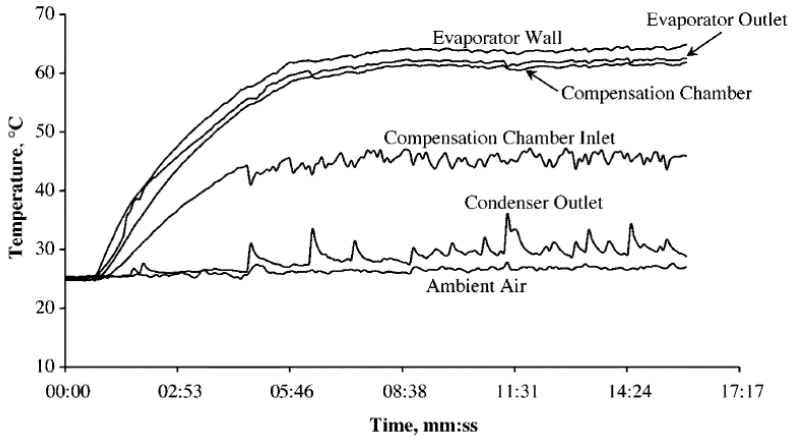

Figure 20. LHP startup test under low heat load of 20 watt (Singh et al., 2007)

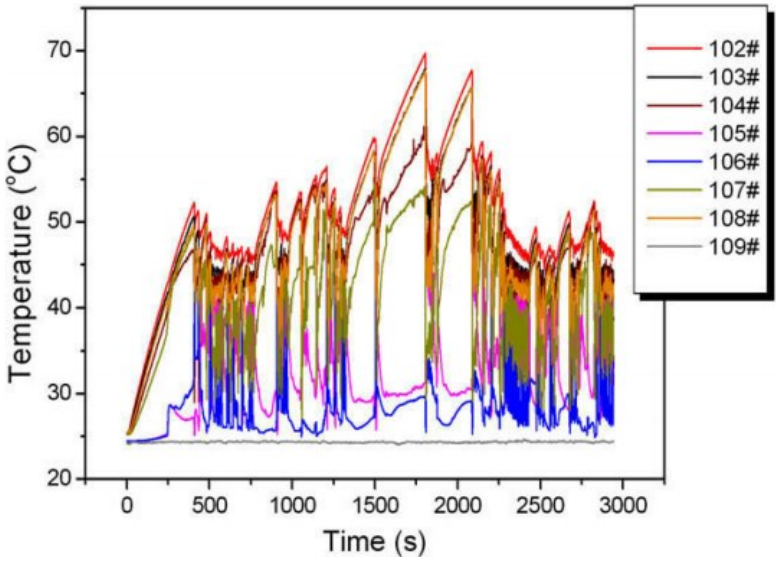

Figure 21. LHP startup process for a 30 watt heat load (Ji Li et al., 2010).

2.11 Effect of Non-condensable Gases

Non-condensable gas (NCG) is one of the most common causes for the heat pipe failure. NCG can occur during the fabrication as well as operational lifespan of the device. The most common source of the generation of NCG inside the loop heat pipe is due to the impurities in fabrication and assembling process and dissolved gases inside the working fluid. Another source of NCG is the incompatibility between the wick and working fluid. The wick and container material used in the device should be chemically compatible with the working fluid at low as well as high temperatures.

Normally, NCG is generated in the evaporation zone. Accumulated gas inside the loop heat pipe can affect its performance. NCG reduce the condensation surface area, which increases thermal resistance. NCG also increase the pressure inside the system, which will increase the evaporation temperature. Liquid absorbing area inside the wick is reduced due to NCG, which causes wick dry out. Experimental study of NCG effects on the LHP operation has been conducted by using ammonia as the working fluid (Nikitkin, Bienert, & Goncharov, 1998). NCG increase the start-up time and the operating temperature.

Figure 22. Oxidation of the container inside the compensation chamber (Singh et al., 2010)

The compensation chamber is the most convenient location for storing the NCG and it reduces loop performance. However, LHP is more tolerable to NCG than traditional heat pipe (Nikitkin et al., 1998) .

2.12 Effect of Gravity (Elevation and Tilt)

The reason for choosing loop heat pipe in space program is the effectiveness of the system in all orientation. Some experiments have been conducted to understand the effect of gravity by changing the elevation and tilt of LHP. LHP elevation refers to position of evaporator with respect to condenser and tilt corresponds to the position of evaporator in reference to the compensation chamber. Adverse elevation means the evaporator is above the condenser and if the tilt is adverse, it refers to evaporator above compensation chamber. Tilt has effects on fluid distribution in compensation chamber and evaporator. Experiment was performed to examine the performance of a LHP for positive and adverse tilts(Kaya & Ku, 1999). The LHP operating temperatures at adverse tilts were much higher than positive tilts for low heat loads. Miniature ammonia LHP can work under all test conditions except for adverse tilts (Chen, Groll, Mertz, Maydanik, & Vershinin, 2006). Though there are some effects of elevation and tilt, operational performance of LHP is excellent than other cooling system and can operate in almost any orientation.

2.13 Heat Transfer Limitations of Loop Heat Pipes

LHP has a number of heat transfer limitations. These limitations can be different in magnitudes and characteristics due to different design of loop heat pipe. For proper design LHP, it is necessary to understand these limitations.

2.13.1 Viscous limitation. If the applied heat load is small, the operating temperature in the system becomes very low. At low temperature, the viscous effects become greater than the

pressure gradients, which cause the fluid to circulate. There is no flow or low flow in the system at this condition and the heat transport capability is limited. This phenomenon is recognized in cryogenic start-up.

2.13.2 Sonic limitation. The vapor velocity in the vapor channel may reach sonic values during the start-up or steady state operation. Under this condition, the maximum mass flow rate can choke in the system.

2.13.3 Capillary limitation. This depends on characteristic of primary wick and working fluid. Both of them can influence the pumping capability to circulate the working fluid in the loop. This limitation is also known as hydrodynamic limit. If the total pressure drops along the system is larger than the capillary pressure developed in the wick structure, the wick dries out and operation of the LHP becomes unstable.

2.13.4 Boiling limitation. For traditional heat pipes, heat travels all the way through the wick structure saturated with liquid and the liquid evaporates in the core area. If the wall temperature becomes excessively high, boiling of the liquid can take place in the wick structure. The vapor bubbles generated inside the wick structure may block the liquid return paths and the wick can dry out. In LHP, the generated vapor bubbles can be vented easily through the vapor channel.

CHAPTER 3

Material and Methodology

3.1 Experimental Setup

A loop heat pipe has been designed and to perform the experiment. One copper wick was fabricated for the loop in the lab and another stainless steel 316 wick was purchased from vendor. Chapter 3 describes the detail procedures and techniques to analyze the characteristic of sintered wicks used in the thermal loop. At First, the process for preparing the samples of wick is presented. Then, the methodology to analyze these properties is discussed. Construction procedures of experimental setup and different parameters applied in the experiment are also explained in detail. Figure 23 shows the schematic of the loop heat pipe for the experiment.

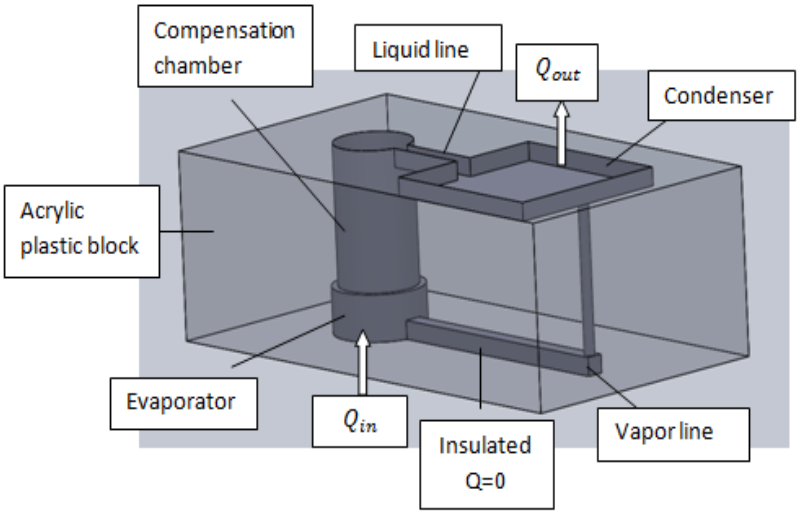

Figure 23. Schematic of loop heat pipe

3.2 Major Components of Loop Heat Pipe

The major components of loop heat pipe (LHP) shown in figure 24 are as follows:

a. Compensation chamber

b. Wick

c. Vapor groove

d. Vapor line

e. Liquid line

f. Condenser

g. Top and bottom aluminum plate

h. Heater block

i. Teflon block to insulate the heater from surrounding environment

j. The charging system

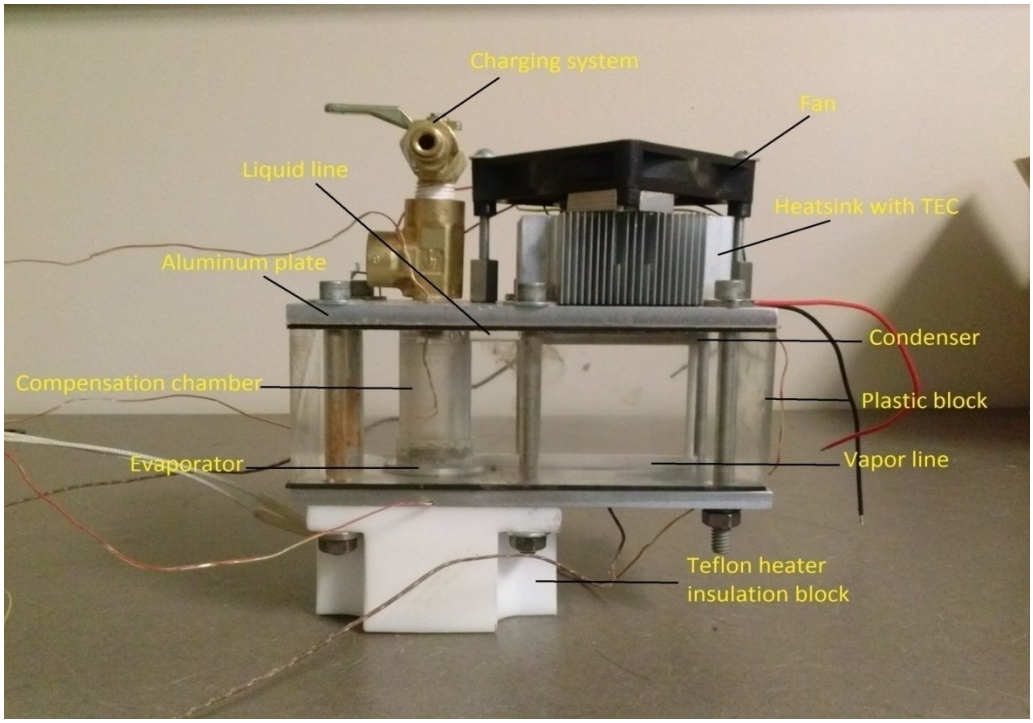

Figure 24. Experimental setup of loop heat pipe

3.3 Manufacturing of Wick

3.3.1 Powder material and particle size. A wick material has been developed from fine copper powder. Fine powder was selected due to fulfill requirement of high capillary pressure. The copper powder was purchased from Alfa Aesar, MA, USA. This powder was spherical in

shape with 10μm diameter. Scanning electron microscope (SEM) is utilized to confirm the size and shape of the particle.

3.3.2 Sample preparation. The samples were prepared in stainless steel mold. The mold used for preparing the sample has diameter of 25.4mm and 7mm depth. The mold is shown in figure 25.

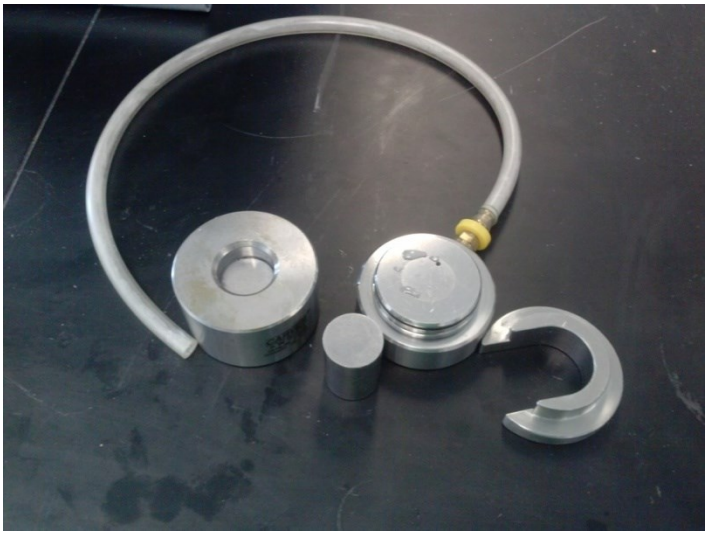

Figure 25. Mold used for preparing the sample

A hydraulic press has been used for cold pressing. After the powder is poured in the mold, the mold has been shaken for uniform distribution of the powder inside the mold. Twelve metric ton hydraulic pressure was applied on the mold to prepare the desired sample. This pressure has been kept for 30 minutes. The diameter of sample is 25.4 mm and the thickness of sample is 3 mm.

3.3.3 Sintering procedure. The samples were loaded in a tube furnace for sintering**.** To avoid the oxidation of the samples, protective atmosphere was maintained during sintering. Pure nitrogen gas was allowed to flow for 1.5 hours to purge the furnace tube. During The purging process, oxygen was diffused out of the pores of the sample. After finishing the nitrogen, purging forming gas was used as the protective atmosphere. The composition of forming gas

used is 4% hydrogen and 96% nitrogen. The flow of forming gas flow started with the start of sintering process.

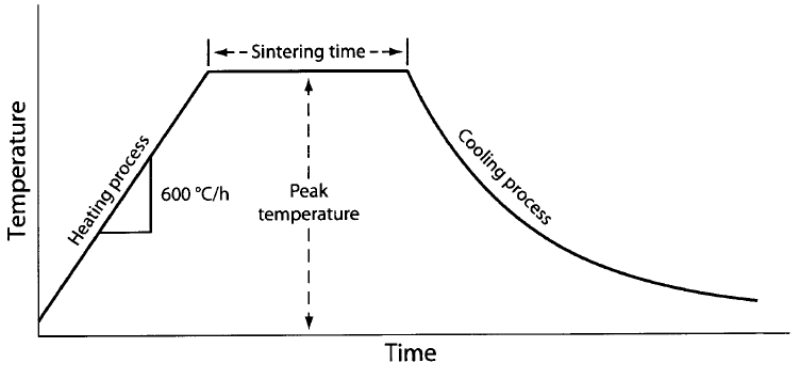

*Figure 26.*Time-temperature plot of the sintering process.

Figure 26 shows a time-temperature plot of the sintering process. The heating rate of 600 °C/h was maintained to reach the peak sintering temperature. The peak sintering temperature was 450 °C. The furnace was held at the peak sintering temperature for 30 minutes. Once sintering was finished, the sinter was cooled inside the furnace. After reaching the temperature bellow 200 °C, the forming gas flow was stopped and only pure nitrogen flow was started. Nitrogen flow was stopped once the sinter reached room temperature.

Figure 27. Sintered Cu wick

The particles bonded together by sintering. Thus, the wick becomes stronger. For proper thermo physical property, samples should be sintered at 450 °C or above. The porosity of sample is calculated from the equation given below

$$\text{Porosity (\%)} = 1 - \frac{\rho_{sample}}{\rho_{material}}$$

Here ρ_{sample} is the density of the sample and $\rho_{material}$ is the density of the pure material. Density of the porous sample was calculated by dividing the mass of the sample by the volume of the sample. A digital balance measured the mass of the sample. The uncertainty in the measurement was 1%.

3.4 Construction of Main Structure of LHP

One of the main objectives of this experiment is to visualize the operating process in LHP. Most of the LHP are made from either copper or stainless steel or from other metallic component. Analytical models are developed without any physical observation of the processes inside the loop. These models cannot provide any comprehensive picture of the system. It is very important to investigate the behavior of the fluid inside the evaporator and in condenser where the phase changes take place. To visualize the processes, main components of LHP is fabricated inside an acrylic plastic block. The schematic of plastic mold is shown in figure. 28.

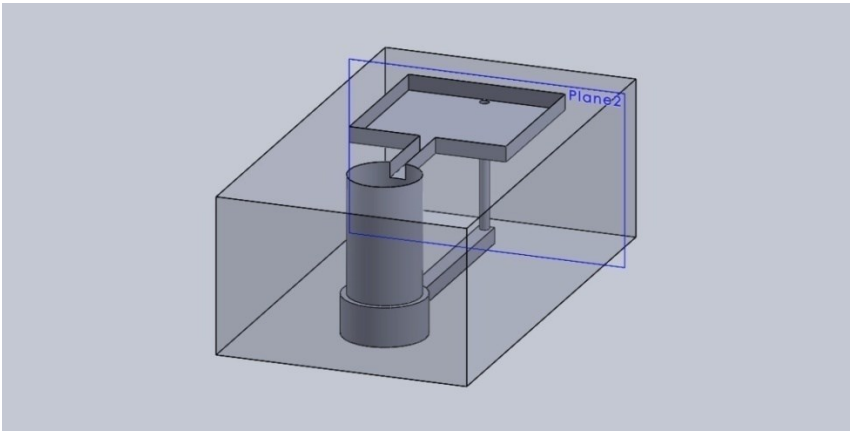

Figure 28. Schematic diagram of the block

The dimension of the block (LxWxH) is 143x80x50 mm. The diameter of the compensation chamber is 22.86 mm and the height of the compensation chamber is 38.5 mm. The evaporator section, which holds the wick, is 26.67 mm diameter and the height of the chamber is 12.5 mm. The volume of the compensation chamber was made equal to the total internal volume of the other component of loop to accommodate most of the displaced liquid from the loop.

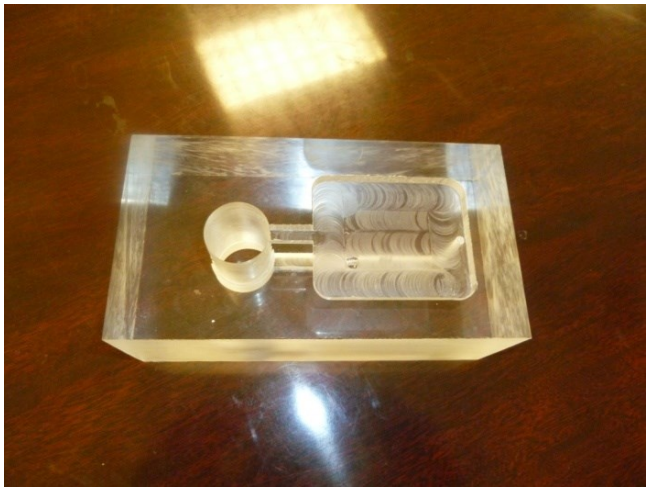

Figure 29. Top view of the main structure of LHP

A condenser with total length of 50 mm and 50 mm width and height of 5 mm depth is formed into the acrylic mold. The condenser was used to reject heat transferred from the evaporator to the ambient air. The condenser was attached with a Thermo Eclectic Cooler (TEC). The TEC has two faces i. e. hot and cold faces. The cold face is connected to the condenser and the hot faced is connected to a heat sink with electrical fan. Detail description of the TEC and heat sink is given later. The rectangular channel of vapor is 5mm width, 5 mm depth and 70 mm long. This channel is connected to a 3mm diameter and 40 mm length line to the condenser and the liquid line is a rectangular channel attached to the compensation chamber. The dimension of the liquid channel is 5 mm width, 5 mm depth and 30mm length. The two-

aluminum plate covers the top and bottom of the mold. The thicknesses of the plates are 6 mm. The length and width of the both the plates are 142.86 mm and 80 mm respectively. On the bottom plate there is a hole of 38.1 mm (1.5 inch) diameter for the heater. Figure 30 shows the bottom view of actual mold machined from acrylic plastic.

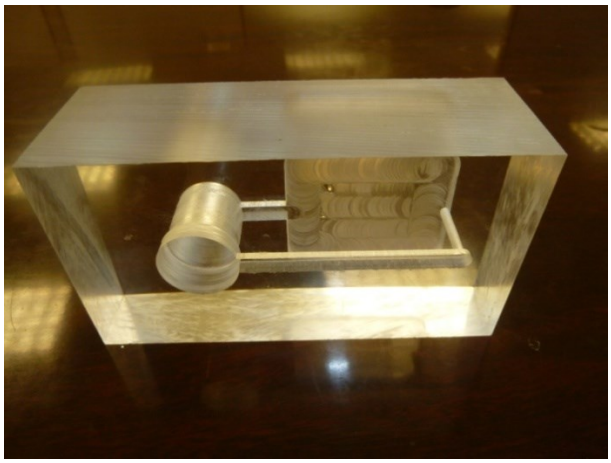

Figure 30. Bottom view of the main structure of LHP

3.5 Vapor Groove

Vapor groove is machined from aluminum, which has high heat conductivity to conduct the heat from heat source to the wick. To remove the vapor produced in the evaporator zone, vapor removal channels is formed by machining 6 very small grooves with rectangular cross-section of 4 mm depth and 1 mm width. The bottom plate of vapor groove plate is 2 mm thick.

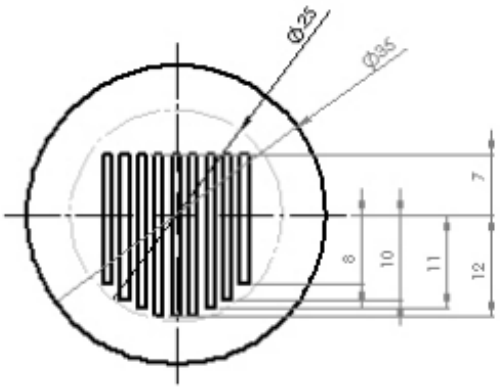

Figure 31. Drawing of vapor groove

To accumulate and remove the vapor, some space is kept (vapor collection zone) in front of vapor groove. Figure 32 shows the vapor removal channel used in the evaporator. The vapor removal channel has two main functions. The fins work as heat conductor between heat source and the wick to generate liquid–vapor interface present in the pores of the wick and the channels assist to remove the vapor to the vapor line.

Figure 32. Aluminum vapor groove

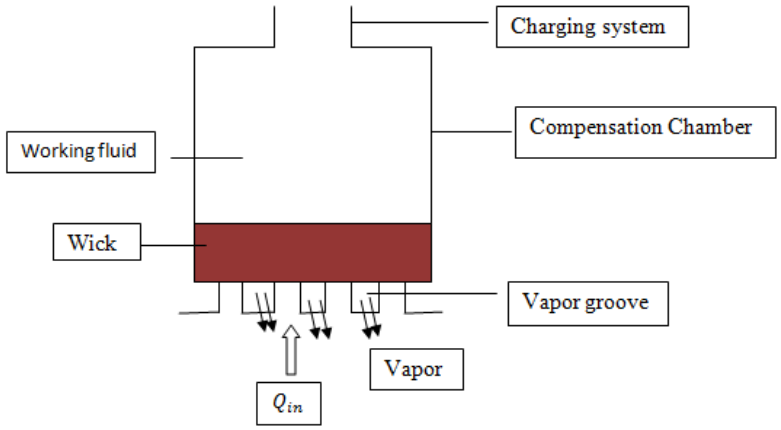

Figure 33. Schematic of vapor groove and wick assembly in LHP

3.6 Working Fluid

Water is used as working fluid in this experiment. Water is used as working fluid is due to high surface tension and good compatibility with wick material. High surface tension will provide more capillary pressure. Thermo-physical properties of water are shown in table 1.

Table 1

Thermo-physical properties of water

Thermo-physical Property	Water
Boiling point (℃) @ 1 atm	100
Liquid density (kg/m^3)	1000
Latent heat of vaporization (kJ/kg)	2270
Specific heat (kJ/kg-K)	4.187
Surface tension (N/m)	0.073
Thermal conductivity (W/m-K)	0.596
Viscosity (kg/m-s)	0.001

3.7 Measuring Instruments

Temperature measurements were performed with six K type thermocouples. Thermocouples are connected to the different locations of LHP to understand the thermal behavior of the loop. Data collection and processing was performed with the help of an IOtech 6000 series data acquisition system. The data acquisition system is connected to a computer. Encore software was used to communicate between the data acquisition system and computer. The experimental setup also consist a high-speed camera and back light illumination unit. Operating process of LHP was recorded through use of a high-speed camera attached to a zoom lens. High-speed camera (Photron USA, Inc., San Diego) was used to capture the images and video of fluid at the different components of LHP. Image-Pro Plus 5.0 software was used to analyze the images. Figure 34 shows the location of thermocouples and table 3.2 presents the specific instruments used for each measured variable.

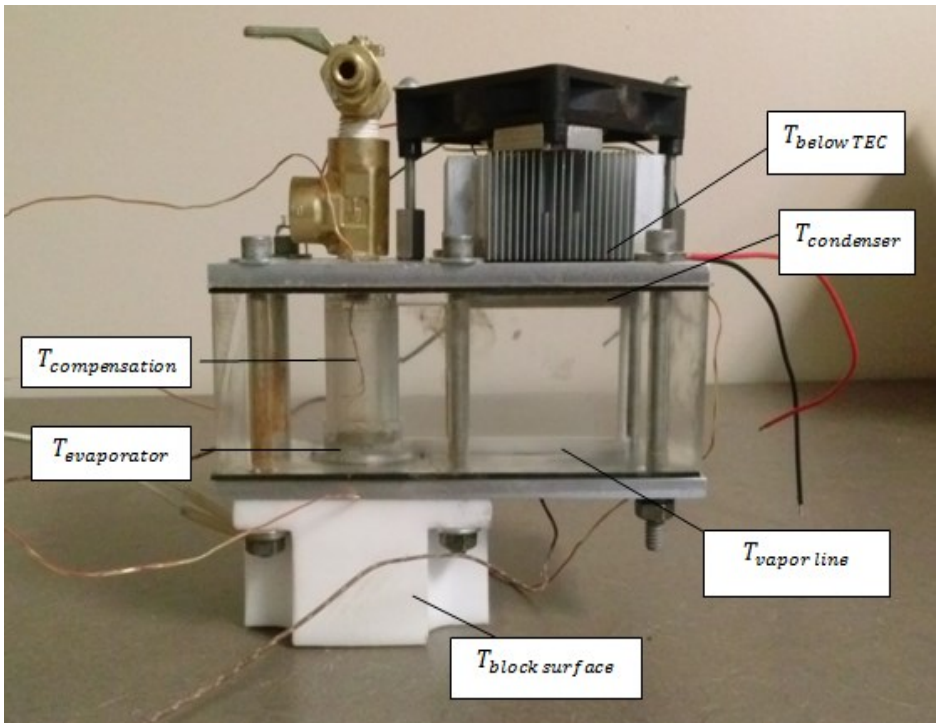

Figure 34. Location of thermocouples in loop heat pipe

Table 2

Measuring instruments

Variable	Instrument
Temperature	K-type thermocouple
Pressure	PX 303A Pressure transducers
Visualization	High speed camera

3.8 Data Acquisition System

An IOtech 6000 series DAQ (Measurement Computing Corporation, MA, USA) is used to collect the measured data. The data was collected at the frequencies between 1-100 kHz. The data acquisition system is connected to a computer. The IOtech Encore software installed at the computer analyzes the data collected. Figure 35 shows the IOtech DAQ system used for the data acquisition for all the measured data.

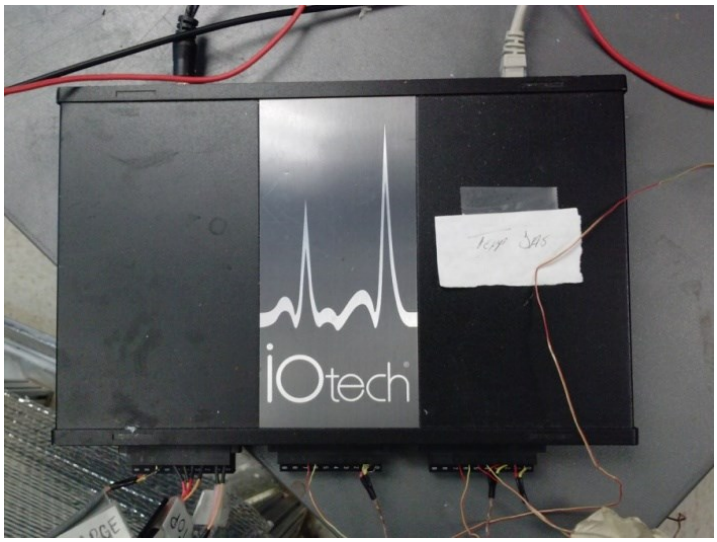

Figure 35. IOtech 6000 data acquisition system

3.9 Heat Flux Measurement

Power to the test specimen provided by the Agilent 6030A voltage supply (Agilent Technologies, 5301 Stevens Creek Blvd, CA 95051, USA). At each voltage, the corresponding current is recorded and the power output is determined. Figure 36 shows the front and rear view of the Agilent 6030A programmable power supply.

Figure 36. Agilent 6030A programmable power supply

Heat losses are minimized by the careful construction considerations of the experiments. To minimize the heat loss from the heater block to the surrounding, at first a ceramic block and

late a PTFF Teflon block are used for insulation. A K-type thermocouple is used to measure the temperature of the surface o the heater block.

3.10 Heater Block

The heater block is made of copper material due to high thermal conductive property of the copper. The diameter of cylinder heater block is 31.75 mm (1.25 inch) and the length is 38.1 mm (1.5 inch). To accommodate the heater cartridge, a 6.35 mm (0.25 inch) of hole is in the heater block. Schematic of the heater block is shown in figure. 37.

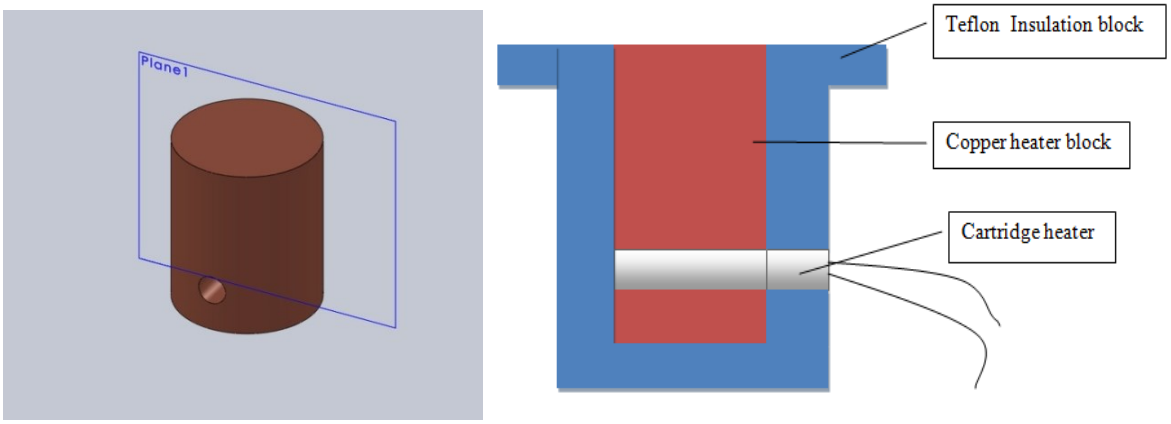

(a) (b)

Figure 37. Schematic of (a) heater block (b) cross section of insulation and heater block assembly

A high-density 150-watt cartridge heater is inserted in the heater block. A programmable power supply is connected to the cartridge heater. When heating a block with high density heater cartridge, fit is an important issue for performance and life expectancy of the heater. Fit is the clearance between the diameter of the hole and diameter of the cartridge heater. Figure 37 shows the picture of the heater block and the cross sectional view of insulator heater blocks assembly. Fit is the difference between the diameter of drill hole and the diameter of the cartridge heater. The recommended fit for the heater is 0.010 inch.

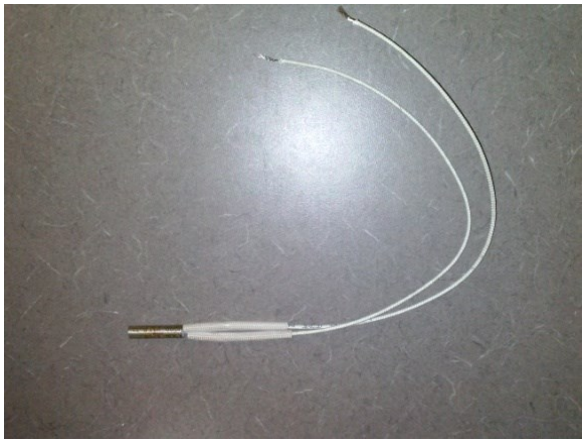

Figure 38. Heater of 150 watt used in the heater block

To minimize the heat loss from the heater to the surrounding, the test specimen is insulated using low thermal conductive machinable ceramic material. Figure 39 shows the first ceramic insulator used in the experiment.

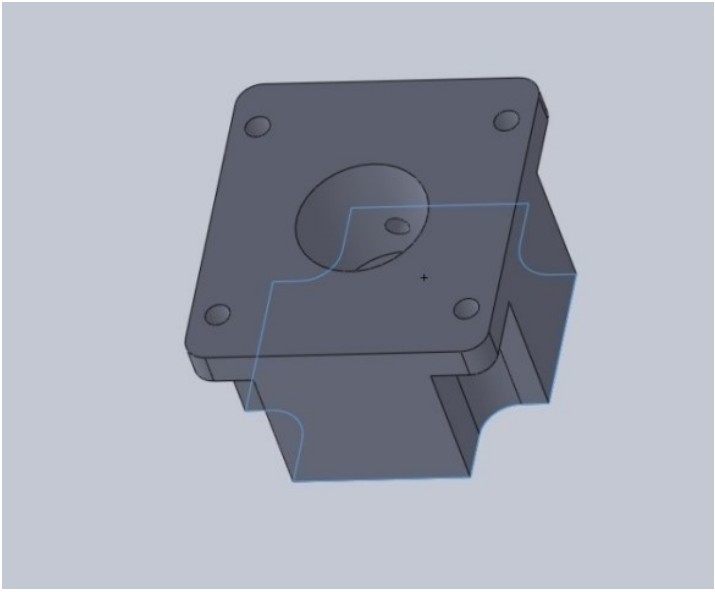

Figure 39. Ceramic block used for insulation of the heater block

At the beginning of the experiment, ceramic block shown in figure 39 was utilized for insulation of the heater block. Heat applied to the heater block is transferred to the evaporator. However, heat loss was found from the ceramic block to the surrounding environment. To resolve the problem, another insulating block of Teflon® PTFE resins has been used in the

experiment. This material is chemical resistance and can perform in high temperature (up to 500°F). The heat loss from the heater block has been reduced after utilizing PTFF. The Teflon block is shown in figure 40.

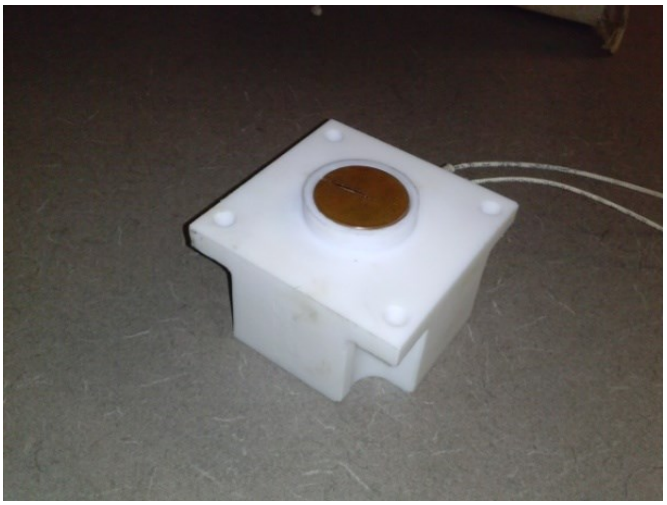

Figure 40. PTFF Teflon block for heater block insulation

Two high temperature gaskets were used for insulation and to prevent the any leakage from LHP to the surrounding environment. If the total system is insulated, the heat applied to the evaporator will be transferred to the condenser. The heat input in the evaporator and the heat rejection in the condenser will be close. Packing was also used around the circumference of the wick to prevent any internal leaks of vapor to the compensation chamber and to minimize heat conduction from the evaporator sidewalls to the wick structure. Surface contact between the wick and vapor channel were checked to ensure proper contact.

3.11 Condenser

Normally the condensation process is performed by liquid coolant circulation or by air. The condensation process is a challenge for the system. For condensation, a rectangular chamber of 50 mm length and 50 mm width and 5 mm depth was formed on the top of the acrylic mold but later the depth has been reduced to 1 mm. Schematic of the top plate is shown in figure 41.

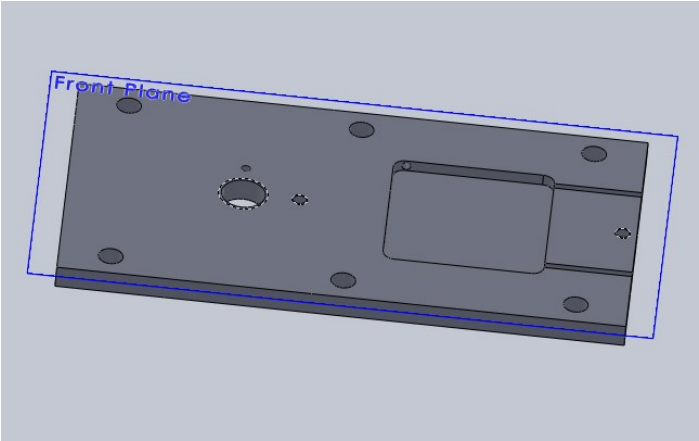

Figure 41. Schematic of top plate of LHP

The condenser is utilized to condense the incoming vapor into liquid phase. A Thermo Electric Cooler (TEC) achieves the condensation process. The TEC is place in the aluminum plate. TEC is very small in shape and needs only electric supply to operate. The cooling can be controlled more accurately than by conventional air or liquid cooling systems. Thermoelectric cooling uses the Peltier effect between the junctions of two different types of materials. A Peltier cooler transfers heat from one side of the device to the other, with consumption of electrical energy. Cooling can be controlled very accurately because of the electric controlling of the cooling system Figure 42 shows a TEC of LxWxH of 50x50x3.2 mm respectively.

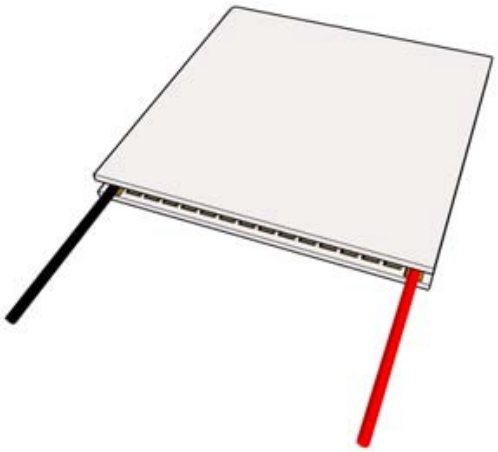

Figure 42. Schematic of TEC

Table 3

The specification of TEC

Part no.	I_{max}(amp)	Q_{max}(watt)	V_{max}(volt)	DT_{max}(℃)	T_{max}(℃)
19911-5L31-15CQ	15.5	225	24	64	125

The cooling capacity can be controlled by a DC power supply. To observe the cooling effect in the condenser, power supply of TEC was varied as per manufacturer specification, which is shown in Figure 43.

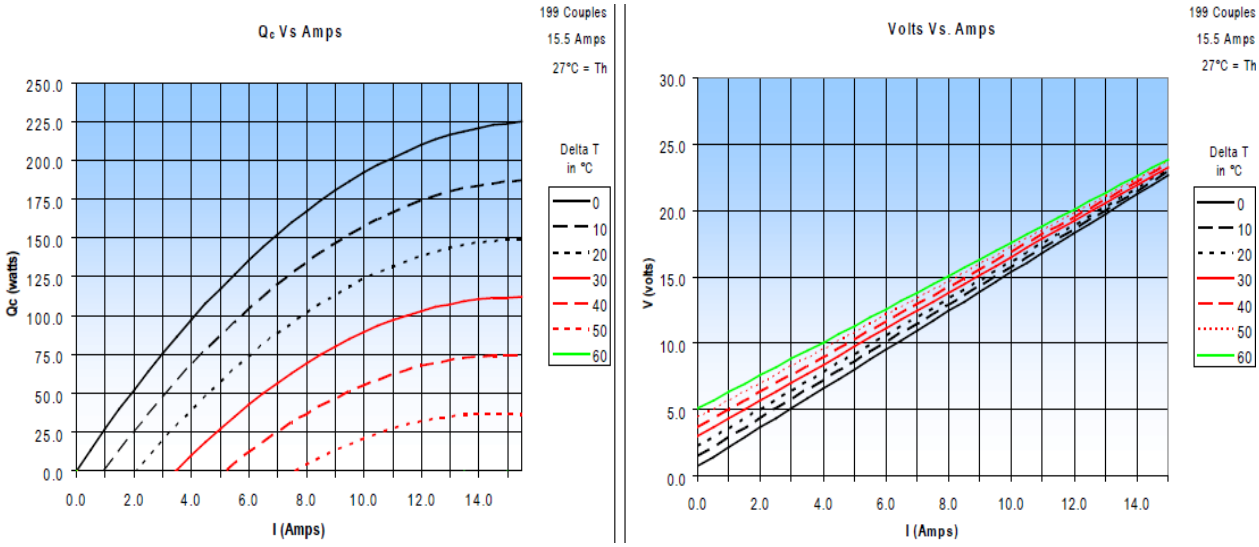

Figure 43. Performance of TEC at different load conditions

The cold face of the TEC will provide the cooling effect and the heat will be move from the bottom face of TEC to the top face. Contact between the plate and the TEC is ensured by using a high conductive thermal silicon paste. The heat from the hot face of TEC is removed by a heat sink of Aluminum fin. On the top of the heat sink, a DC electric fan is used to remove the heat from the heat sink to environment by convection. Figure 44 shows the heat sink used on top plate.

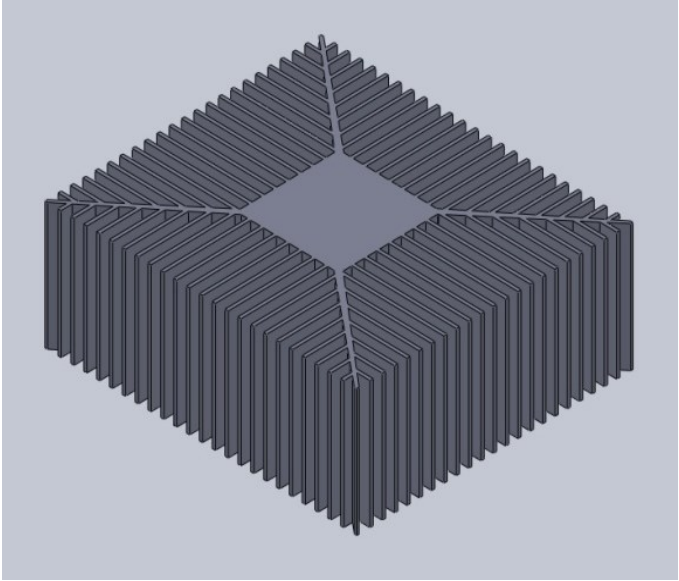

Figure 44. Heat sink used on the top of TEC

3.12 Non Condensable gases

Non-condensable gases can be produced during the fabrication and operation process of loop heat pipe. Mostly non-condensable gases (NCG) are generated from the impurities through fabrication and machining process. Another source of NCG is dissolved gases in the working fluid. If the working liquid and loop wick material or container is not compatible, then NCG can be generated inside the LHP.

NCG reduce the surface area for condensation, increase the thermal resistance inside the loop, and loop saturation temperature. NCG also increase pressure drop inside the system. NCG accumulate over the surface area of wick and hinders the normal supply of liquid into the pores of wick which may causes dry out of the wick. If the generation of NCG is too high, it may completely stop the operation of LHP.

Cleaning is essential for minimizing NCG. Careful procedures were followed to avoid machining leftovers. The cleaning was done by using acetic acid (CH3COOH). De-ionized water is used to clean the surfaces.

A special charging system has been designed for charging the liquid and the loop. A three-way valve is attached upon the top plate of LHP. One port of three-way valve is connected to a vacuum pump and the other port is connected to the liquid charging cylinder. All the ports are connected to common port of compensation chamber of the loop.

Figure 45. Vacuum pump for charging system

Before charging the liquid, the port connected to the vacuum pump is open end to vacuum the loop. The vacuum pressure create inside the loop is of 8 psig. A pressure gauge is connected to the third port of three-way valve to read the pressure inside the loop during vacuum operation. The suction side of the vacuum pump is connected to the vacuum port of the charging system and the delivery port of the vacuum pump is open to the atmosphere. Figure 45 shows the vacuum pump.

To avoid NCG formation cooled deionizer water used to remove vapor bubble. The amount of water charged inside the loop heat pipe is 50% or higher of the volume of compensation chamber. Figure 46 shows the three-way valve used in charging process used in the loop.

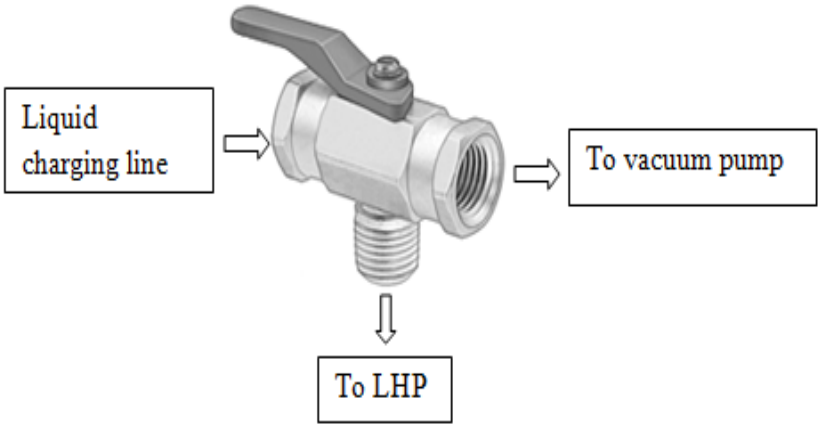

Figure 46. Schematic of charging system of LHP

3.13 Heat Transfer Analysis

Heat transfer analysis has to be done to understand the operational effectiveness of the LHP. Heat flux is applied uniformly to the evaporator. Part of the applied heat is utilized for evaporation of the liquid in the wick and the rest of the applied heat goes to the compensation chamber and this portion of heat also known as heat loss from the system. So it can be written:

$$Q_{applied} = Q_{evap} + Q_{heat\ loss}$$

Heat loss takes place from the metallic structure of the LHP and in compensation chamber. However, the main structure of the loop is made from acrylic plastic and special attention is given for insulation of heater block. The main heat loss takes place in compensation chamber. It is difficult to minimize the heat loss to compensation chamber. The conductivity of the wick can affect the heat loss to the compensation chamber. Stainless steel wick has low thermal conductivity. It ensures minimum heat loss to compensation chamber.

3.14 Analysis of Pressure Balance

The total pressure drop of the loop is the sum of the pressure drops in each component of the loop and can be written as:

$$\Delta P_{cap\ max} \geq \Delta P_{wick} + \Delta P_{cond} + \Delta P_{vapor\ line} + \Delta P_{liquid\ line}$$

Maximum operating pressure is obtained from the evaporating menisci formed at the pore of the wick. Capillary limit of the loop depends on the wick design and the pressure developed can be expressed by Young-Laplace equation as:

$$P_{cap\ max} = \frac{2\sigma cos\theta}{r}$$

Where σ is the surface tension of working fluid, θ is the contact angle between the liquid and solid, and r is the pore radius of the wick.

For steady-state operating condition, the capillary pressure gain in the wick must be balanced by the pressure loss in each component. The pressure drops in the system can be defined in three categories. Those are

a. The pressure drop in single phase (liquid and vapor line)
b. The pressure drop in two phase (in condenser)
c. The pressure drop in wick itself

Already mentioned single phase takes place in the grooves just below the wick, in the vapor and liquid transport lines. The single-phase pressure drop can be calculated from Darcy-Weisbach equation, which is

$$\nabla P = f\left(\frac{l}{d_h}\right)\left(\frac{\rho v^2}{2}\right)$$

Here *f* is a dimensionless number, which is known as Darcy friction factor and is depend upon Reynolds number and roughness of the tube. For laminar flow in smooth circular pipe, f can be calculated from the equation

$$f\ \text{Re}=64$$

For turbulent flow, the value of friction factor can be calculated from another solution proposed by H. Blasius and the equation is as follows

$$f = 0.316Re^{-0.25}$$

The Reynolds number can be calculated by the following equation

$$\text{Re}=\frac{\rho v l}{\mu}$$

Where ρ is density of the liquid, v is the velocity of the liquid and l is the effective length of the system and μ is the viscosity of the liquid.

Flow in the vapor grooves is also laminar. The Reynolds number in the vapor groove can be calculated by the hydraulic diameter of the groove. The hydraulic diameter can be calculated as follows

$$d_h = \frac{2h_{groove}w_{groove}}{(h_{groove} + w_{groove})}$$

For this loop heat pipe $h_{groove} = 2\ mm$ and $w_{groove} = 1\ mm$

Now Darcy friction factor can be estimated from the proposed equation f Re=57. Reynolds number can be calculated as mentioned above. Single-phase flow is assumed to prevail along the grooves, in the vapor and liquid transport lines and through the porous wick. The single-phase viscous pressure drop in the porous wick can be estimated from the Darcy-Weisbach equation,

$$\Delta P = \frac{m\mu_l l_w}{\rho_l A_w K_w}$$

m= mass flow rate

μ_l =Viscosity of liquid

l_w= length of the wick

ρ_l= density of the liquid

A_w= area of the wick

K_w= permeability of the wick

The pore diameter in wick is one of the important factors to provide capillary pressure in LHP. Higher capillary pumping pressure can be achieved by small pore diameter. However, it increases the pressure drop in the wick. The Darcy's law for porous media as mentioned above can express the pressure drop inside the wick.

It is difficult to define the length of two phases in the condenser. The vapor enters the condenser in the saturated state and the vapor turns into liquid phase. The vapor cannot immediately change from vapor phase to liquid phase. There is a time lag in between these two phases. Two phase exist in the condenser. For the ease of the calculation, the calculation of the pressure drop of the condenser can be done by assuming only single phase i.e. either the liquid phase or vapor phase pressure drop. The highest-pressure drop of the two can be assumed as the pressure drop the condenser. The worst possible scenario can calculate maximum pressure drop inside the condenser.

CHAPTER 4

Results

4.1 SEM Images of Wick Structure

Scanning electron microscope (SEM) was used to observe the microstructure of both the copper and stainless steel wicks. Figure 47 shows the microstructure of stainless steel wick at 100X magnification. It is evident from the figure; the particles are not spherical for stainless steel wick.

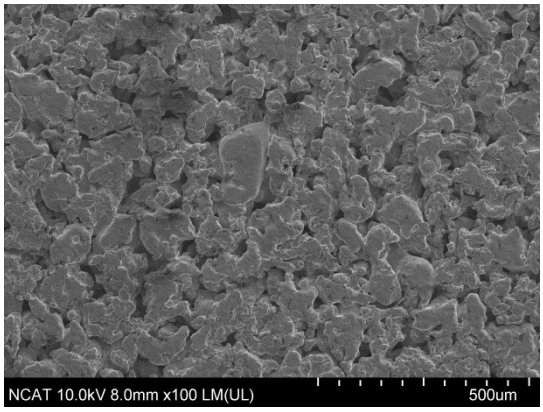

Figure 47. SEM images of stainless steel at 100X magnification

Figure 48 shows the SEM images of copper power and sintered copper wick

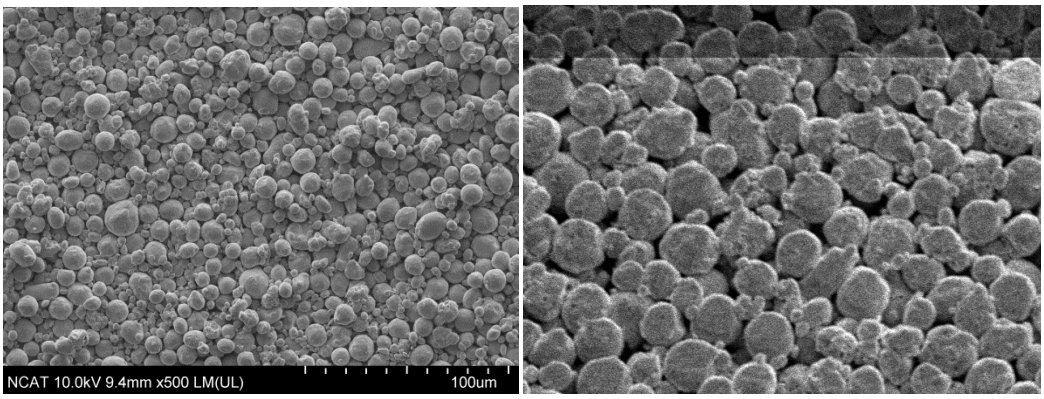

(a) (b)

Figure 48. SEM images of (a) copper powder at 500 X magnification (b) microstructure of sintered copper wick

From figure 48, it is obvious that the shape of the particle is spherical and the average diameter is approximate $10\mu m$. The second image is the microstructure of the sintered wick of copper.

4.2 Porosity:

Porosity is defined as the ratio of the volume of the voids to the total volume. After preparing the samples, a slide caliper measured the dimensions of the samples and a digital balance measured the mass of the sample. These measurements are used to calculate the porosity. The porosity of sample is calculated from the equation given below

$$\text{Porosity } (\%) = 1 - \frac{\rho_{sample}}{\rho_{material}}$$

Here ρ_{sample} is the density of the sample and $\rho_{material}$ is the density of the pure material. Density of the porous sample was calculated by dividing the mass of the sample by the volume of the sample. The porosity of copper wick is 30% and porosity of stainless steel wick is 40%. The uncertainty in the measurement of porosity was 1%.

4.3 Thermal Analysis of LHP

The temperature was measured at different points of LHP by using K-Type thermocouples shown in table 1. Six thermocouples have been used to read the temperature profile at the different component of the system. These thermocouples are directly connected to IOtech 6000 series DAQ data acquisition system. The data acquisition system collects the data after every 0. 5 sec and display the data on the computer connected to acquisition system. Encore software that communicates between the DAQ and the computer CPU. Error in temperature measurement by K type thermocouples is ±0.1 °C. Power to the test specimen is provided by the Agilent 6030A programmable voltage supply. Uncertainty in the power measurement is ±0.2 percentage.

Table 4

Position of thermocouples

Serial Number	Location of thermocouple	DAQ channel number
1	Condenser	CH 5
2	Vapor line	CH 8
3	Compensation Chamber	CH 9
4	Evaporator	CH 10
5	Below TEC	CH 11
6	Outside of heater block insulator	CH 12

4.3.1 Startup process and steady state condition. Figure 49 shows the startup process for 20-watt heat load. At low heat input, heat leakage to the compensation chamber and to the environment is large. It takes several minutes to start up the system due to low power input. The generation of the vapor bubble is very small in number at low heat load.

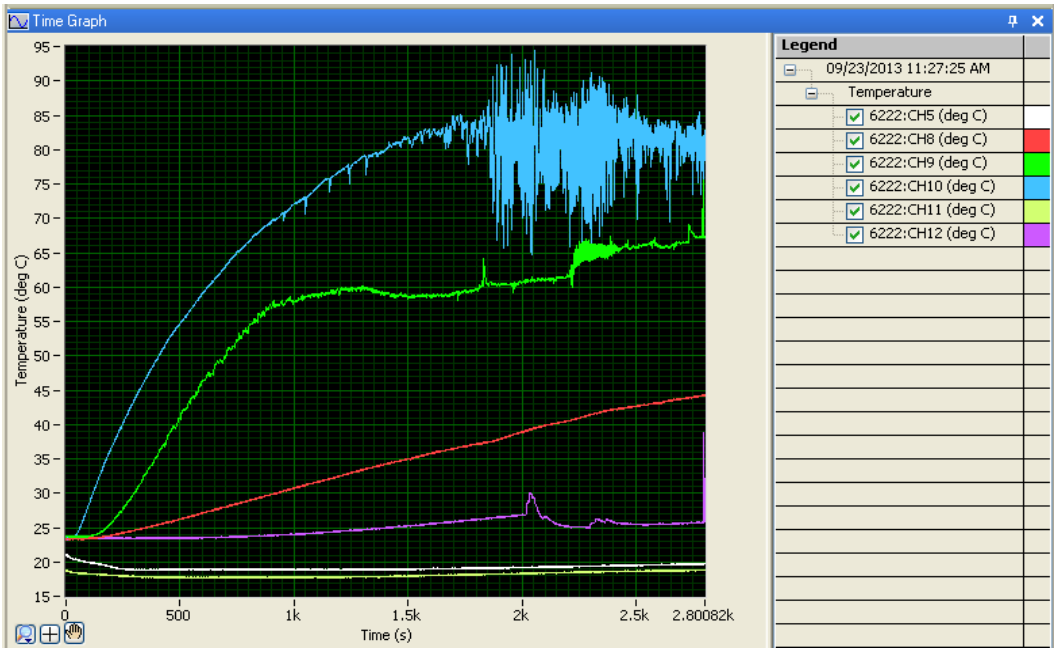

Figure 49. LHP startup process with 20-watt heating power

It can be noticed from the figure 49, there is a sudden high temperature oscillation at the evaporator after approximately25 minutes when the evaporator temperature reaches almost 85°C. The range of this oscillation is about 30 °C (65 to 95°C). The reason for chaotic oscillation is the irregular vapor generation. Chaotic oscillations of temperature can be observed also in compensation chamber. Inconsistent return of condensed liquid to the compensation chamber may cause the fluctuation in temperature.

Figure 50 shows the startup process for 30-watt heat input power. The heat load is higher than previous one. Still the heat load is relatively low. The oscillation of temperature can be observed in evaporator, compensation chamber and vapor line.

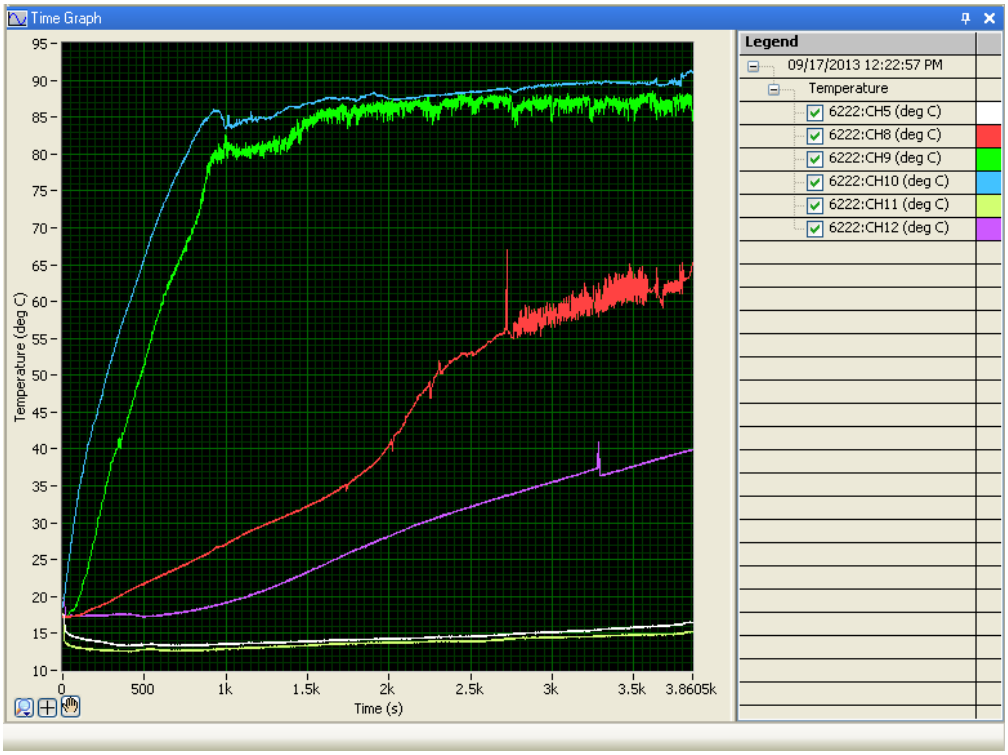

Figure 50. LHP startup process with 30-watt heating power

During the startup process, the vapor line is flooded with water. Vapor generation and collapsing of bubble can cause the oscillation until the vapor line is free of liquid. The temperature oscillation for compensation chamber starts at about 85°C. The range of oscillation

is about 5 ℃ in compensation chamber. The chaotic behavior in compensation chamber continues until the continuous return from the condenser. Temperatures of both the TEC and the Condenser are below 20℃ during the operation.

Start of the loop heat pipe at low power input have been observed by Ji Li et al. (2010). Singh et al. (2007) have mentioned two start-up processes. Ji Li et al. (2010) have mentioned the possible reason for the chaotic behavior is alternative vaporization and flooding in the porous wick. This causes the instability of meniscus form in the wick. Existence of two-phase can also create the oscillation.

Startup process is more stable for 50-watt heat load than the 30-watt startup process. The evaporator temperature rises very quickly and bubble generation becomes more faster than two previous cases

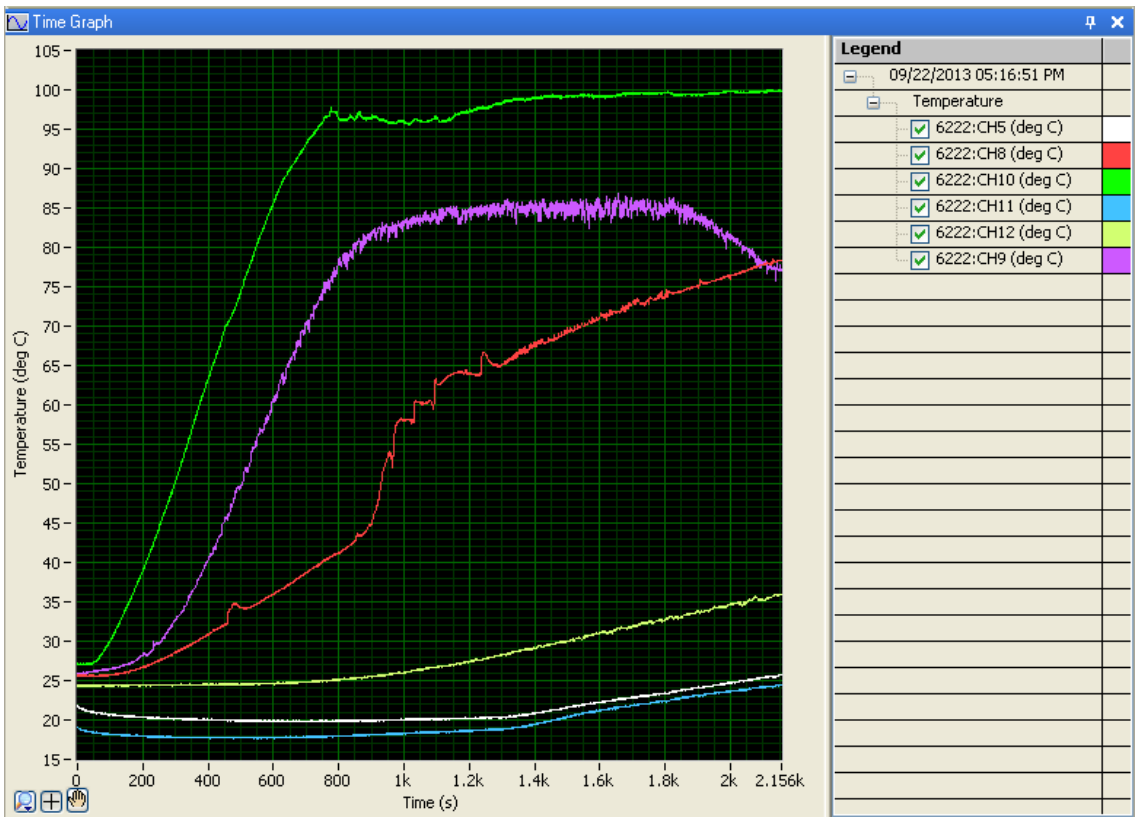

Figure 51. LHP startup process with 50-watt heating power

The temperature of the compensation chamber gets the stability at 85℃. A decrease in the compensation chamber temperature was observed lather. The temperature dropped from 85℃ to 78℃. the temperature dropped due to high amount of condensate coming into the compensation chamber. The temperature of compensation chamber became stable again after the drop.

The effects of adding working fluid in the compensation chamber can be found in figure 52. The heat load in the evaporator is 60 watt. The evaporator, compensation chamber and vapor outlet temperature ascend very quickly. Liquid is added to the compensation chamber through charging system after compensation chamber reaches 80℃. The effect of adding new liquid can be noticed by large temperature drop of the compensation chamber. The temperature drops to approximate 52℃. The temperature of compensation chamber became stable later. There is some spike in the condenser temperature profile. Collapse of vapor bubble in the condenser may cause the spike in temperature.

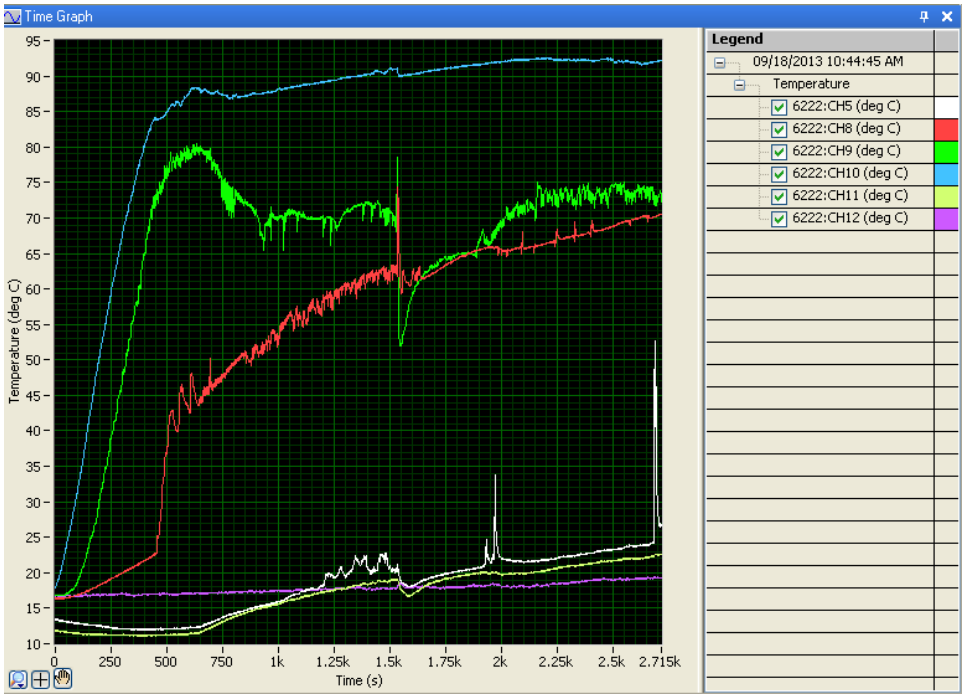

Figure 52. LHP startup process with 60-watt heating power

Figure 53 presents the temperature profile for the startup of 90 watt. Most stable temperature profile was observed for 90-watt heat load. High oscillation of temperature can be seen at the beginning of evaporation. Though the vapor outlet temperature increased, the other temperature profiles of LHP demonstrated the steady state behavior. LHP starts very quickly for the higher heat load. It can be shown that stable operation mode can be accomplished at relatively high heat load with negligible fluctuations in the temperature curves. There is a slight increase both in the temperature of the TEC and condenser. Ji Li et al. (2010) have also mentioned similar temperature profile for loop heat pipe at 300 watt.

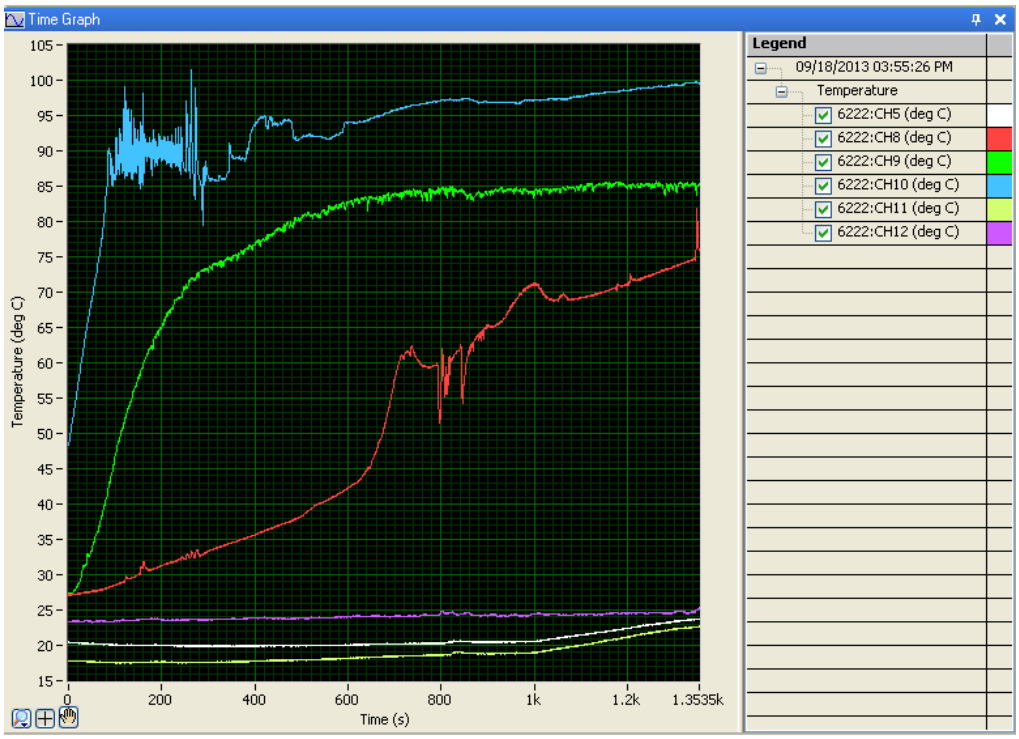

Figure 53. LHP startup process with 90-watt heating power

Higher power input of 100 watt was applied to evaporator. The response of the system can be viewed at figure 54. The evaporator temperature keeps rising and at approximately 32 minutes the temperature shoot to a higher value. The vapor line temperature shows the same trend and keeps climbing

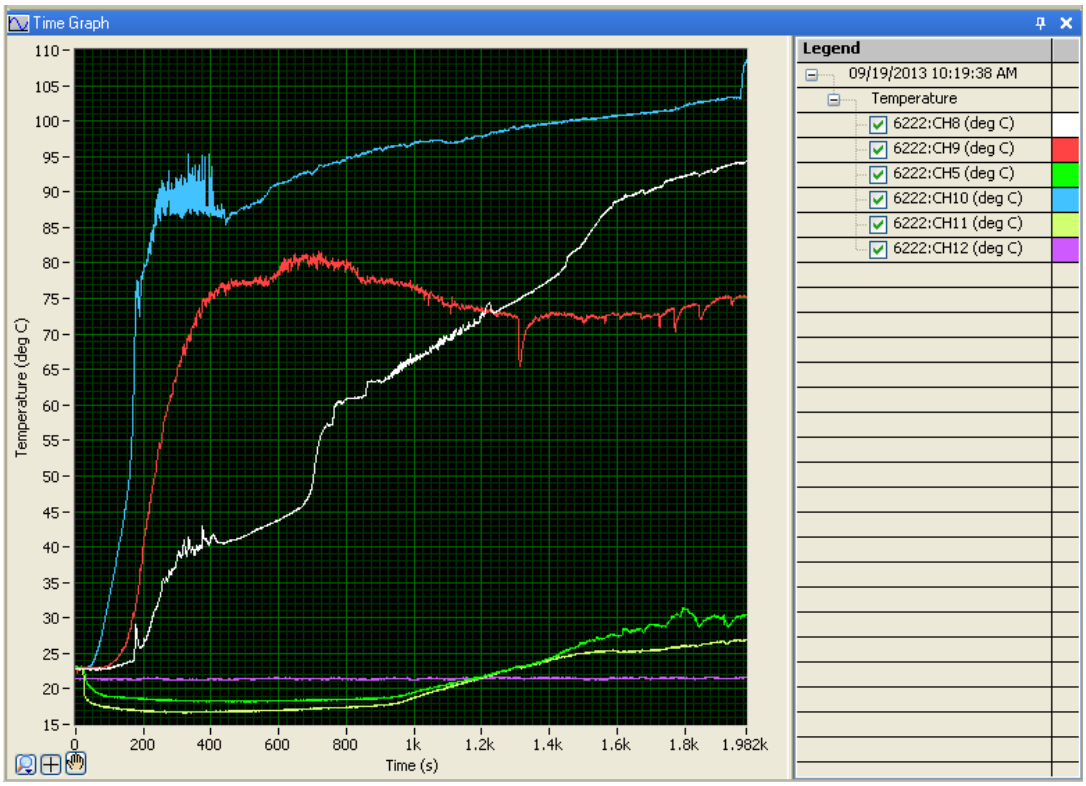

Figure 54. LHP startup process at heat load of 100 watt.

The compensation chamber remains almost stable. However, the condenser temperature increases at a moderate rate after 16 minutes.

Step load is applied to the system to see the system behavior. Heat load was applied after a certain time interval and the system response was observed with every change in heat load. Figure 55 illustrate the response of the system at different time interval at wide range of power input in the evaporator. Comparatively low power input of 20 watt was applied to the system at the beginning. The power input was gradually increased to 100 watt. The temperature rise was slow at the beginning for the evaporator temperature. The temperatures rise quickly with the increase of heat input. The vapor outlet temperature kept rising with the heat load. Condenser and TEC temperatures were almost steady until a certain period. High level of oscillation was found in the condenser at 100 watt.

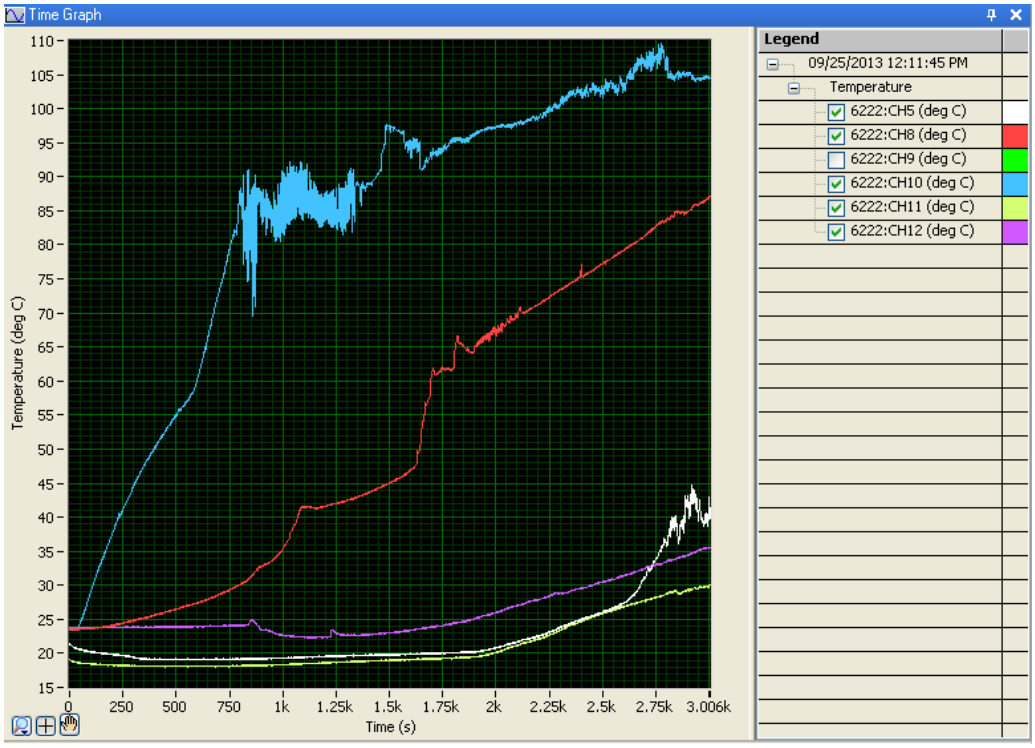

Figure 55. Effects of gradual increase in heat load

4.3.2. Thermal resistance. One of the important parameter for determining the performance of a loop heat pipe is the thermal resistance. Total thermal resistance can be defined as

$$R_{th} = \frac{(T_e - T_c)}{Q}$$

where T_e is the temperature at the evaporator, T_c is the temperature at the condenser and Q is the applied load at the evaporator. The thermal resistance provides the idea of resistance of the system to heat flow. The thermal resistance should be low for the efficient system. The total thermal resistance of the LHP at different load is shown in figure 56. The thermal resistance is high at low heat load but the resistance decreases with higher heat load. Heat leakage to the compensation chamber is high at the low heat load. Most of the applied load is lost to the heat leakage to compensation chamber and to the environment. The system starts up very quickly at

higher heat load due to low thermal resistance. Effects of thermal resistance was also observed by Singh et al. (2007). They have demonstrated that total thermal resistance decreases with heat load.

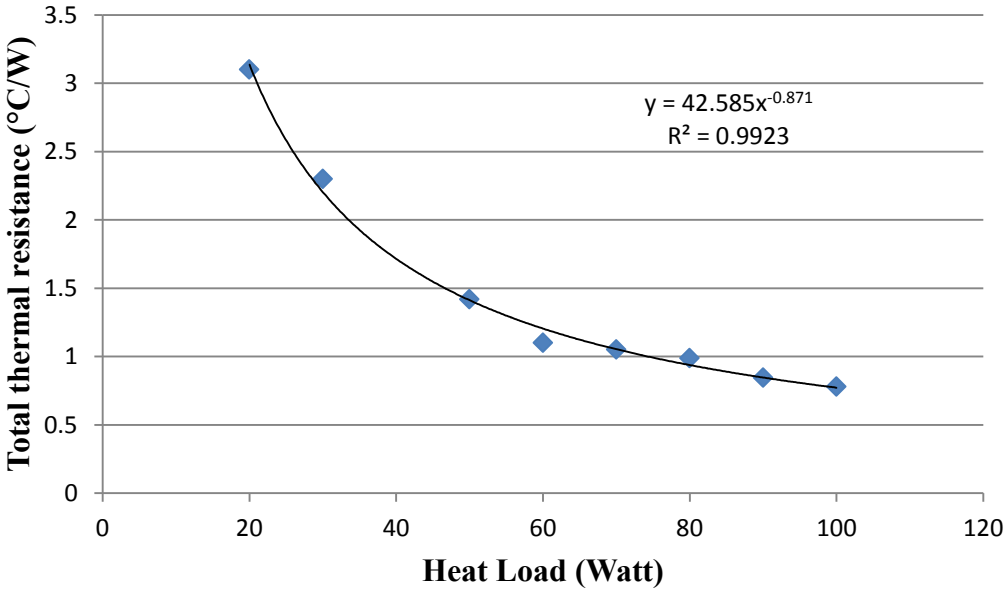

Figure 56. Total thermal resistance vs. heat load.

Evaporator is the most significant component of the LHP and can determine the overall performance of the device. One of the important factors for determining system performance is evaporator thermal resistance. Evaporator thermal resistance is the resistance encountered at the evaporator. It is preferred thermal resistance decreases with heat load. It is evident from the figure 57, evaporator thermal resistance decrease with heat load. The evaporator thermal resistance is low when the load is 60 watt to 100 watt. This can be also observed at the temperature response graphs discussed earlier. This range is the efficient region where the system is stable. The resistance is lower 0.2 $℃/W$ at the heat load of 100 watt. The result of evaporator thermal resistance can be also compared to the Singh et al. (2007) who have also explained the similar characteristic for their system.

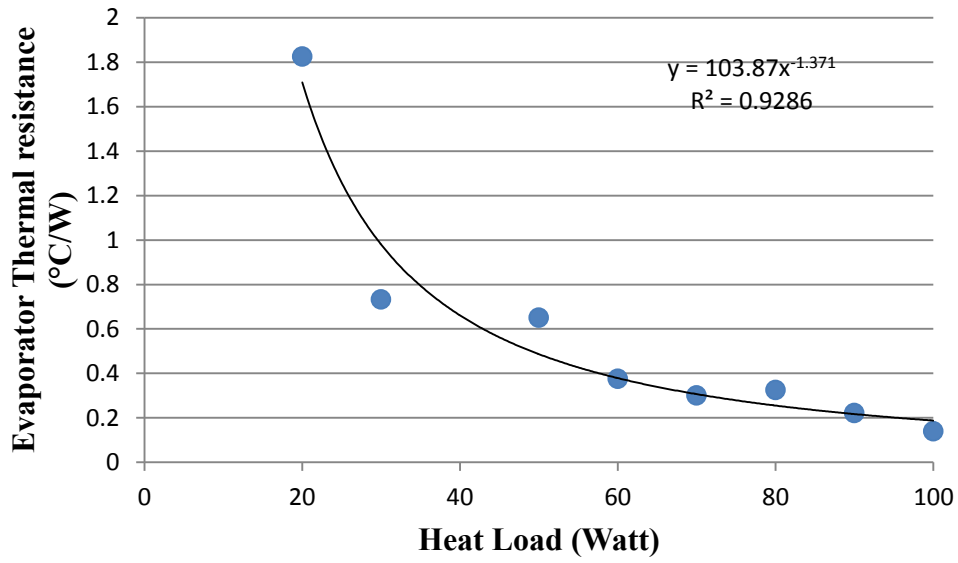

Figure 57. Evaporator thermal resistance vs. heat load

4.3.3 Heat transfer coefficient. The designed LHP is capable of cooling efficiently high heat fluxes without any concern in the performance. The efficiency of any heat exchange system can be determined by the heat transfer coefficient. For a competent system, the value of heat transfer coefficient should be high. The heat transfer coefficient can be calculated as follows

$$h = \frac{Q}{A_e(T_e - T_V)}$$

where Q is the applied load on the evaporator, A_e active heated area of the evaporator, T_e is the temperature of the evaporator and T_V is the temperature of the vapor outlet. Figure 58 illustrate heat transfer coefficient at different heat loads. Maximum heat transfer coefficient in the evaporator is 14 KW/m^2°C for 100 watt. The plot clearly indicates that high values of the heat transfer coefficient can be achieved at relatively high heat loads. The heat transfer coefficient should be higher and the thermal resistance should be lower for high heat loads. The minimum value of heat transfer coefficient is 1.08 KW/m^2°C for 20 watt. Yury F Maydanik et al. (2005) have shown the same trend in the heat transfer coefficient at different heat loads. They

have shown that heat transfer coefficient increases for working fluid water with the increase in heat load.

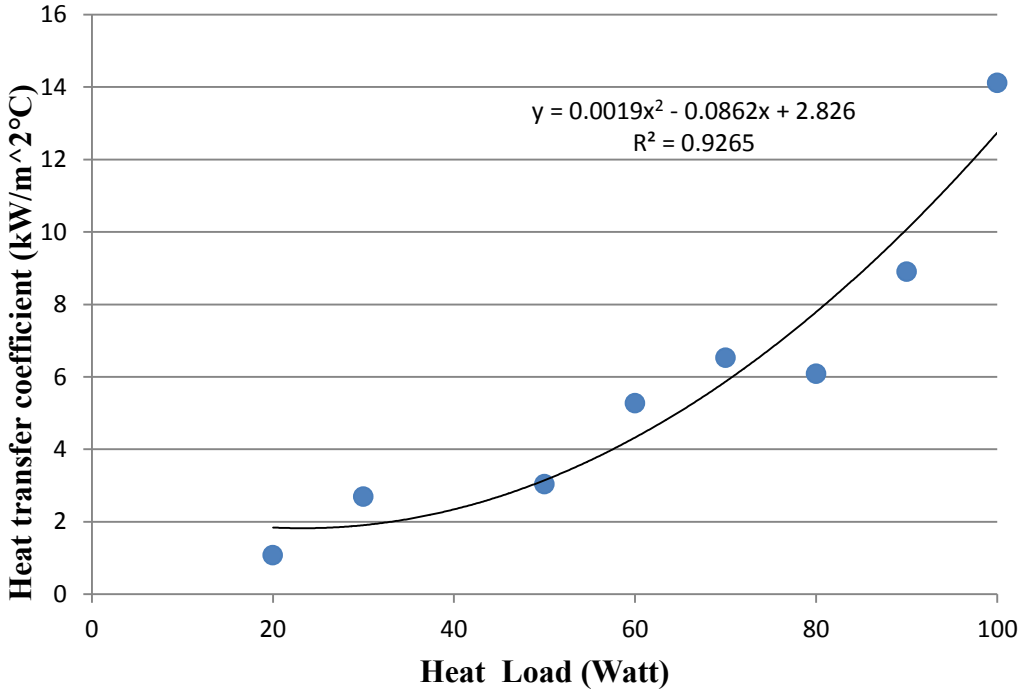

Figure 58. Evaporator heat transfer coefficient vs. heat load

4.3.4 Transient behavior of LHP. Condenser is one of the key components of LHP. Heat transfer efficiency depends upon the performance of condenser. In the experiment, TEC has been used for condensation process. The performance of the condenser should be stable for all heat loads. It is expected that condenser temperature should be low even at the high heat load applied to the system. The temperature of the condenser at different power input is shown in figure 59. The figure demonstrates that condenser temperature increases with different heat power input. For the high heat load of 80 to 90 watt, the condenser temperature at the end of the operation is maximum 31 to 32℃. At high heat load, high generation of vapor increases condenser temperature. The maximum temperature of the condenser is within 35℃ , which indicate reasonable performance of LHP.

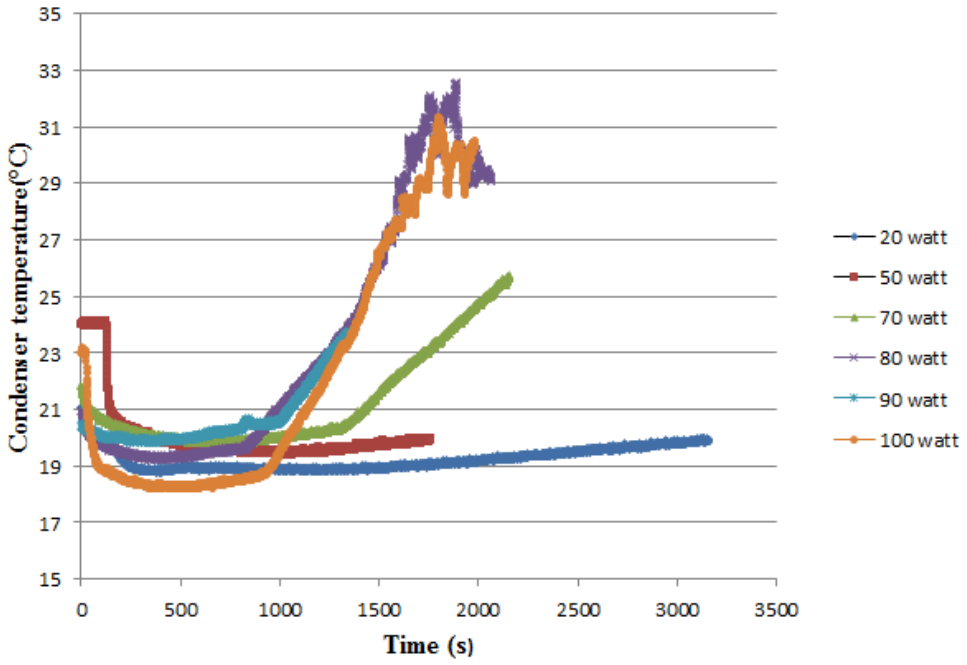

Figure 59. Condenser temperature vs. time at different heat load

Figure 60 shows condenser maximum temperature at every load condition during the operation after the system gets steady state condition. The temperature kept rising with the rise of the power input. The temperature curve of the condenser becomes steady at around 32°C for the heat load of 80 to 100 watt.

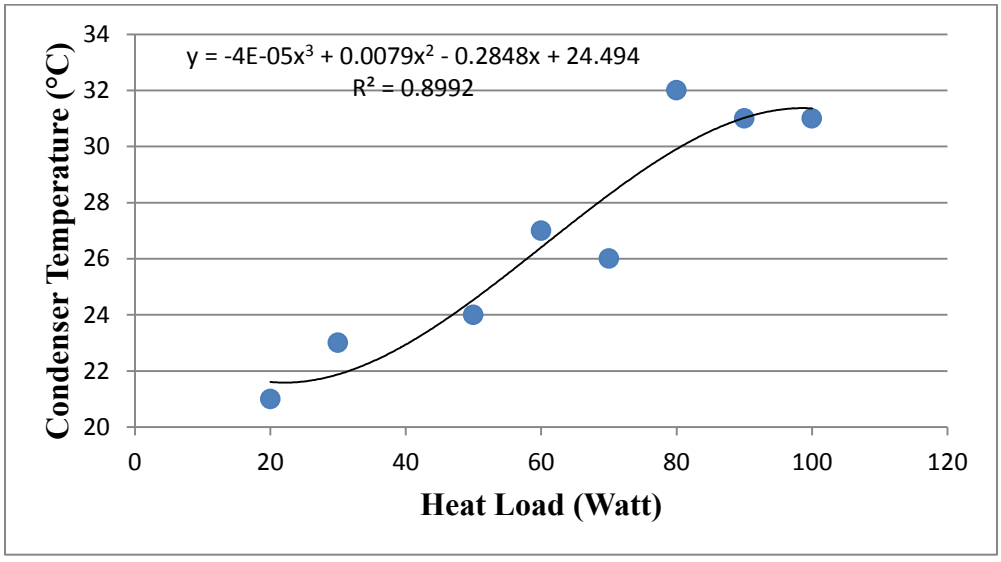

Figure 60. Condenser temperature at different heat load

Evaporator contains the wick which separate the two phase of the fluid. The evaporator dictates the startup process and the steady state condition. Figure 61 illustrates the temperature profile of the evaporator at different heat loads during the operation period. High oscillation of the temperature can be seen at low heat load of 20 watt. The rate of temperature rise increases with the rise in power input. It takes longer time to start the vapor generation for the low heat input of 20 watt. The system reaches the vapor generation temperature very quickly for the high heat load. The start of vapor generation is very quick and then it reaches the steady state temperature of approximate 100℃ for the heat load of 90 and 100 watt. The temperature oscillation can be found very rapidly due to faster vapor generation for high heat load. A temperature jump can be observed for 100 watt but for the other cases the system gets steady with the progress of time. The slope of the evaporator temperature curve increases with the increase of heating load

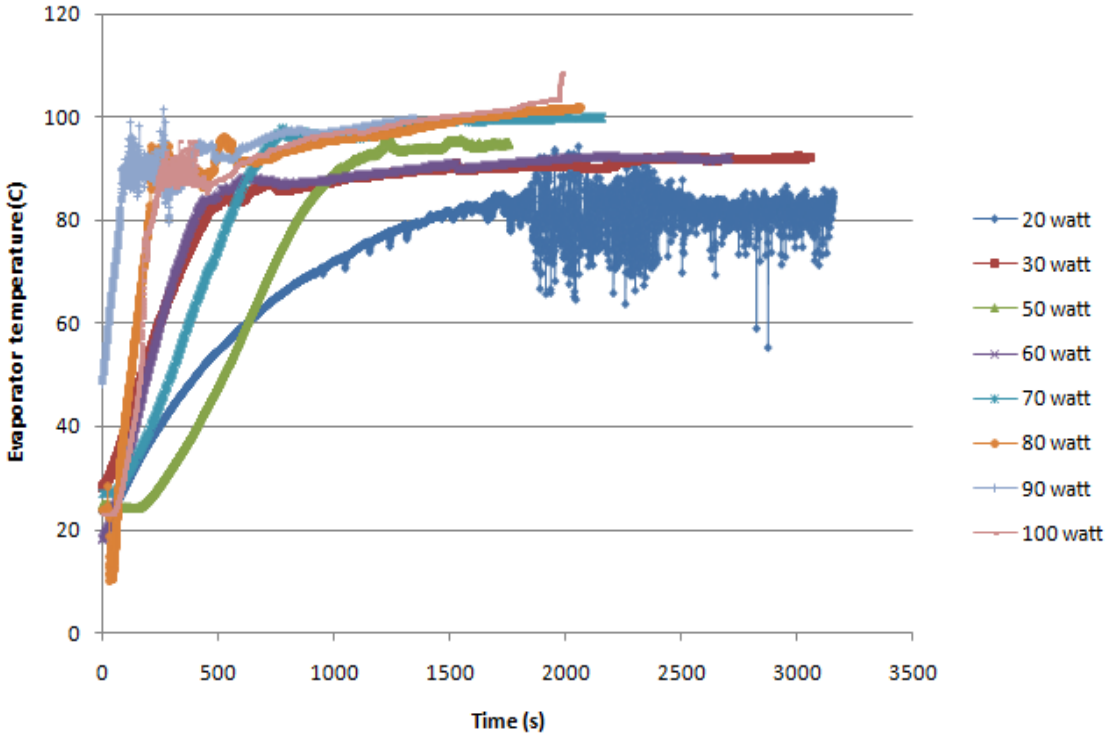

Figure 61. Evaporator temperature at different heat loads

4.4 Visualization of LHP

Jun and Woei (2011) have explained the starting process of LHP into four stages. The generated vapor-bubble drives out the liquid out of groove and vapor at the beginning of the startup. The meniscus is not stable and cause temperature oscillation. Startup process can be observed in figure 62. The vapor front moves forward and drive the liquid out of vapor line

At the second stage, vapor grooves are free of liquid. The vapor drives the vapor line toward the condenser. During this stage, still there is some temperature oscillations but moderate than the previous one.

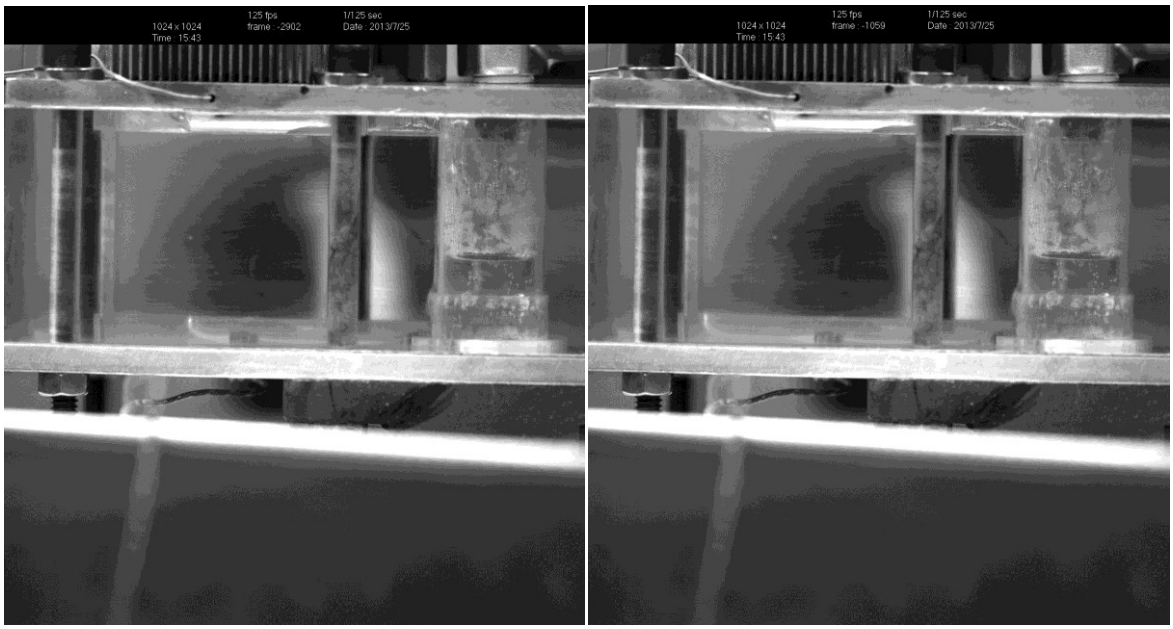

Figure 62. Advancement of vapor in the vapor line during startup

During the stage three, there is no liquid in the vapor line. The vapor generated in the evaporator directly comes to the condenser. As soon as the vapor comes to the condenser, the heat exchange takes place and the vapor turns into liquid. After the condenser is filled up with the liquid, vapor bubbles creates a continuous pressure waves in the condenser due to the two-phase instabilities. Bubble forms inside the condenser are shown in figure 63. The rate of bubble formation is increased with heat load.

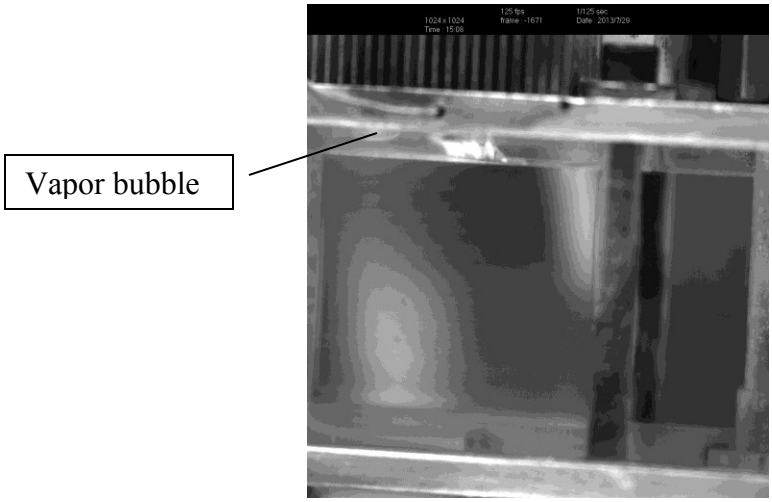

Figure 63. Two phase mixture in the condenser

In the stage 4, the condensed liquid returns into the compensation chamber. At the beginning, the rate of return is inconsistent but after some periods, the flow becomes consistent. Heat leaks from the evaporator to the compensation chamber and two-phase fluid exists in the chamber. Bubble form inside the compensation chamber along with wick and on the surfaces of the chamber with the rise of temperature. The cold liquid from condenser balances the heat leakage to the compensation chamber. The formation of bubble inside the evaporator is shown in figure 64. Bubble formation in the compensation chamber increases with increase in heat load.

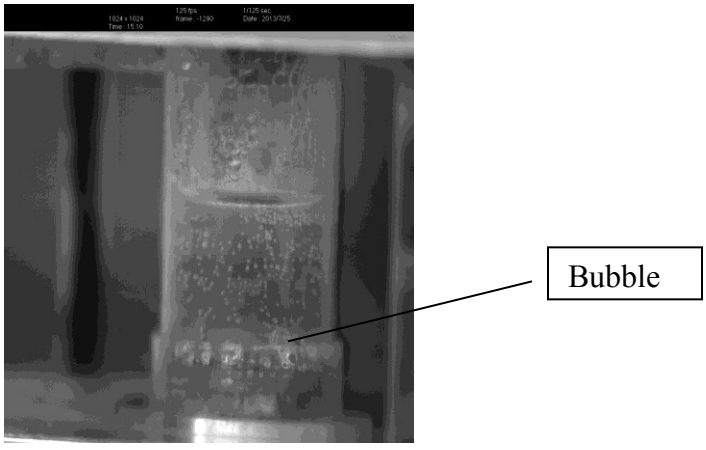

Figure 64. Formation of bubble in compensation chamber

CHAPTER 5

Conclusion and Future Research

An experiment has been conducted on loop heat pipe during the present study. Result of the experiment includes the development and evaluation of the performance of LHP at different heat load condition. Numerous tests were performed to study the transient operation of LHP. The current technique provides the opportunity to observe the fluid behavior in the loop. Images taken by the high-speed camera illustrate the startup process as well as behavior of fluid in different component. Understanding of these phenomena will help to improve the efficiency of the loop. The specific goals have been accomplished mentioned in chapter 1. The outcome of the experiment can be concluded as follows

- A LHP has been designed and developed with disc shape wick. The main structure of the LHP is constructed from the acrylic plastic and the working fluid is water.
- LHP was able to handle 100-watt heat load with the total thermal resistance of 0.78 $℃/W$ and heat transfer coefficient of 14.114$W/m^2℃$. The most stable condition was observed for 90-watt heat load. Total thermal resistance for this load is 0.844$℃/W$ and heat transfer coefficient is 8.9 $W/m^2℃$.
- Temperature oscillation was observed in the loop heat pipe during startup and at low heat load. Chaotic behavior of the temperature has been noticed for 20 and 30 watt. The reason for the huge oscillation is instability of the meniscus.
- A high-speed camera was used to visualize the operational behavior of the LHP. Four main stages of the startup process have been analyzed with the help of visualization process. The reasons for temperature oscillation in the evaporator and in the condenser were confirmed through the visualization process. Images taken by the high-speed

camera verify heat leakage to the compensation chamber, existence of the two-phase flow in the condenser and development of bubble in the compensation chamber at the high heat load.

- The manufactured LHP can operate satisfactorily at relatively high heat load. The system is compact and can be used for the cooling of electronic devices.

Though the present study provides an insight into the operational characteristic of LHP, future research needs to be done for improvement in efficiency. Recommendation for the future research is sighted below

- Measurement of pressure at the different components of LHP will give insight into pressure drop along the system.
- Decrease in the working temperature of the system is possible by using various working fluids. Working fluid like ammonia, ethanol can be used for low operating temperature.
- Measurement of the flow rate and vapor quality
- Investigation of two-phase instability in condenser can improve the condensation process.
- Development of a CFD code will help to understand the transient model of LHP more effectively.

References

Altman, EI, Mukminova, M Ia, & Smirnov, HF. (2002). The loop heat pipe evaporators theoretical analysis. Paper presented at the Proceedings of the 12th International Heat Pipe Conference.

Bartuli, E, Vershinin, S, & Maydanik, Yu. (2013). Visual and instrumental investigations of a copper–water loop heat pipe. International Journal of Heat and Mass Transfer, 61, 35-40.

Baumann, Jane, Cullimore, Brent, Yendler, Boris, & Buchan, Eva. (1999). Noncondensible gas, mass, and adverse tilt effects on the start-up of loop heat pipes. Paper presented at the International Conference On Environmental Systems.

Bienert W.B., Krotiuk W.J., Nikitkin M.N. (1999). Thermal control with low power miniature loop heat pipes. Paper presented at the 29th Int. Conf. Environ. Syst., Denver, CO.

Boo, JH, & Chung, WB. (2004). Thermal performance of a small-scale loop heat pipe with PP wick. 13th IHPC, Shanghai, China, 21-25.

Brocheny, Pascal O. (2006). Modeling of the transient behavior of heat pipes with room temperature working fluids. Clemson University.

Cao, Yiding, & Faghri, Amir. (1994). Conjugate analysis of a flat-plate type evaporator for capillary pumped loops with three-dimensional vapor flow in the groove. International journal of heat and mass transfer, 37(3), 401-409.

Chen, Yuming, Groll, Manfred, Mertz, Rainer, Maydanik, Yu F., & Vershinin, S. V. (2006). Steady-state and transient performance of a miniature loop heat pipe. International Journal of Thermal Sciences, 45(11), 1084-1090.

Cheung, KH, Hoang, T, Ku, J, & Kaya, T. (1998). Thermal performance and operational characteristics of loop heat pipe (NRL LHP). SAE paper(981813), 3-16.

Chuang, Po-Ya Abel. (2003a). An improved steady-state model of loop heat pipes based on experimental and theoretical analyses: ProQuest.

Chuang, Po-Ya Abel. (2003b). An improved steady-state model of loop heat pipes based on experimental and theoretical analyses. (3333999 Ph.D.), The Pennsylvania State University, United States -- Pennsylvania. Retrieved from http://search.proquest.com/docview/305314416?accountid=12711 ProQuest Dissertations & Theses Full Text database.

Cimbala, John M, Brenizer, Jack S, Chuang, Abel Po-Ya, Hanna, Shane, Thomas Conroy, C, El-Ganayni, AA, & Riley, David R. (2004). Study of a loop heat pipe using neutron radiography. Applied radiation and isotopes, 61(4), 701-705.

Cytrynowicz, Debra, Hamdan, Mohammed, Medis, Praveen, Shuja, Ahmed, Henderson, H Thurman, Gerner, Frank M, & Golliher, Eric. (2002). MEMS loop heat pipe based on coherent porous silicon technology. Paper presented at the AIP Conference Proceedings.

d'Entremont, BP, & Ochterbeck, JM. (2008). Investigation of Loop Heat Pipe Startup Using Liquid Core Visualization.

Faghri, Amir. (1995). Heat pipe science and technology. Paper presented at the Fuel and Energy Abstracts.

Figus, C, Bray, Y Le, Bories, S, & Prat, M. (1999). Heat and mass transfer with phase change in aporous structure partially heated: continuum model andpore network simulations. International journal of heat and mass transfer, 42(14), 2557-2569.

Gaugler, R. S. (1944). 2350348. U. S. P. a. T. Office.

Grover, G. M., Cotter, T. P., & Erickson, G. F. (1964). Structures of Very High Thermal Conductance. Journal of Applied Physics, 35(6), 1990-1991.

Hoang, Triem T, O'Connell, Tamara A, Ku, Jentung, Butler, C Dan, & Swanson, Theodore D. (2003). Miniature loop heat pipes for electronic cooling.

Jun, Xiang, & Woei, Shyy. (2011). Thermal Performances of Loop Heat Pipe with Hybrid Wick Structures in Evaporator. Paper presented at the 10th IHPS, Taipei, Taiwan.

Kaya, Tarik, & Ku, Jentung. (1999). Ground testing of loop heat pipes for spacecraft thermal control. Paper presented at the 33rd Thermophysics Conference, Norfolk, VA.

Ku, Jentung. (1999). Operating characteristics of loop heat pipes. SAE transactions, 108(1), 503-519.

Ku, Jentung, Ottenstein, Laura, Rogers, Paul, Cheung, Kwok, & Powers, Edward I. (2001). Investigation of low power operation in a loop heat pipe.

Launay, S., and Mekni, N. (2010). Specifically Designed Loop Heat Pipe for Quantitative Characterization. Paper presented at the 15th International Heat Pipe Conference, Clemson, USA.

Lee, WH, Park, KH, & Lee, KJ. (2004). Study on working characteristics of loop heat pipe using a sintered metal wick. 13th IHPC, Shanghai, China, 21-25.

Li, Ji, Wang, Daming, & Peterson, GP. (2010). Experimental studies on a high performance compact loop heat pipe with a square flat evaporator. Applied Thermal Engineering, 30(6), 741-752.

Li, Jinwang, Zou, Yong, Cheng, Lin, Singh, Randeep, & Akbarzadeh, Aliakbar. (2010). Effect of fabricating parameters on properties of sintered porous wicks for loop heat pipe. Powder Technology, 204(2), 241-248.

Liu, Zhichun, Gai, Dongxing, Li, Huan, Liu, Wei, Yang, Jinguo, & Liu, Mengmeng. (2011). Investigation of impact of different working fluids on the operational characteristics of miniature LHP with flat evaporator. Applied Thermal Engineering, 31(16), 3387-3392.

Maidanik Y.F., Vershinin S.V., Chernysheva M.A. (2000). Development and Tests of Miniature Loop Heat Pipe with a Flat Evaporator.

Maidanik, Yu F, Solodovnik, Nikolay, & Fershtater, Yu G. (1995). Investigation of dynamic and stationary characteristics of a loop heat pipe. Paper presented at the IX International Heat Pipe Conference, Albuquerque, New Mexico.

Maydanik, Y.F. (2004). Miniature Loop Heat Pipes. Paper presented at the 13th International Heat Pipe Conference, Shanghai, China.

Maydanik, Yu F. (2005). Loop heat pipes. Applied Thermal Engineering, 25(5), 635-657.

Maydanik, Yury F, Vershinin, Sergey V, Korukov, Mikhail A, & Ochterbeck, Jay M. (2005). Miniature loop heat pipes-a promising means for cooling electronics. Components and Packaging Technologies, IEEE Transactions on, 28(2), 290-296.

Mo, Songping, Hu, Peng, Cao, Jianfeng, Chen, Zeshao, Fan, Hanlin, & Yu, Fei. (2006). Effective thermal conductivity of moist porous sintered nickel material. International journal of thermophysics, 27(1), 304-313.

Moon, Seok Hwan, Hwang, Gunn, Yun, Ho Gyeong, Choy, Tae Goo, & Kang, Young II. (2002). Improving thermal performance of miniature heat pipe for notebook PC cooling. Microelectronics Reliability, 42(1), 135-140.

Nikitkin, Michael N, Bienert, Walter B, & Goncharov, Konstantin A. (1998). Non-condensable gases and loop heat pipe operation. SAE transactions, 107(1), 394-399.

Ogushi, Tetsurou, Yao, Akira, Xu, Jason J, Masumoto, Hiromitsu, & Kawaji, Masahiro. (2003). Heat transport characteristics of flexible looped heat pipe under micro-gravity condition. Heat Transfer—Asian Research, 32(5), 381-390.

Pastukhov V.G., Maydanik Y.F., and Chernyshova M.A. (1999). Development and investigation of miniature loop heat pipes. Paper presented at the 29th Int. Conf. Environ. Syst., Denver, CO,.

Perkins, Jacob. (1836).

Platel, Vincent, Fudym, Olivier, Butto, Claude, & Briend, Philippe. (1996). Coefficient de transfert, à l'interface de vaporisation, d'une boucle fluide diphasique à pompage thermocapillaire. Revue générale de thermique, 35(417), 592-598.

Santos, Paulo HD, Bazzo, Edson, & Oliveira, Amir AM. (2012). Thermal performance and capillary limit of a ceramic wick applied to LHP and CPL. Applied Thermal Engineering, 41, 92-103.

Singh, Randeep, Akbarzadeh, Aliakbar, Dixon, Chris, Mochizuki, Mastaka, & Riehl, Roger R. (2007). Miniature loop heat pipe with flat evaporator for cooling computer CPU. Components and Packaging Technologies, IEEE Transactions on, 30(1), 42-49.

Singh, Randeep, Akbarzadeh, Aliakbar, & Mochizuki, Masataka. (2008). Operational characteristics of a miniature loop heat pipe with flat evaporator. International Journal of Thermal Sciences, 47(11), 1504-1515.

Singh, Randeep, Akbarzadeh, Aliakbar, & Mochizuki, Masataka. (2010). Operational characteristics of the miniature loop heat pipe with non-condensable gases. International Journal of Heat and Mass Transfer, 53(17), 3471-3482.

Stenger, F. J. (1966). Experimental Feasibility Study of Water-Filled Capillary-Pumped Heat Transfer Loops. Paper presented at the NASA TM-X-1310.

Trefethen, L. (1962). On the Surface Tension Pumping of Liquids or a Possible Role of the Candlewick in Space Exploration. Paper presented at the G.E. Tech. Info.

Tu, ZK, Liu, ZC, Liu, C, Gai, DX, Wan, ZM, & Liu, W. (2009). Heat and mass transfer in a flat disc-shaped evaporator of a miniature loop heat pipe. Proceedings of the Institution of Mechanical Engineers, Part G: Journal of Aerospace Engineering, 223(6), 609-618.

Wang, Guanghan, & Nikanpour, Darius. (2007). Visual Observations of Flow and Phase Phenomena in Loop Heat Pipes. Paper presented at the AIP Conference Proceedings.

Wrenn, Kimberly Renee. (2004). Capillary Pumped Loop Performance Investigation Through Flow Visualization.

Yao W., Miao J. , Shao X. (2004). Parametric analysis on LHP/CPL evaporator performance and critical heat flux by two-dimensional calculation. Paper presented at the 13th IHPC, Shanghai, China.

Yeh, Chien-Chih, Chen, Chun-Nan, & Chen, Yau-Ming. (2009). Heat transfer analysis of a loop heat pipe with biporous wicks. International Journal of Heat and Mass Transfer, 52(19), 4426-4434.

Zhao, TS, & Liao, Q. (2000). On capillary-driven flow and phase-change heat transfer in a porous structure heated by a finned surface: measurements and modeling. International Journal of Heat and Mass Transfer, 43(7), 1141-1155.